Rigorous treatment of the $\mathcal{S}^1/\mathbb{Z}_2$ orbifold model with brane-Higgs couplings

Ruifeng Leng,[*] Grégory Moreau,[†] and Florian Nortier[‡]
[1]*Université Paris-Saclay, CNRS/IN2P3, IJCLab, 91405 Orsay, France*

(Received 25 January 2021; accepted 16 March 2021; published 12 April 2021)

We build rigorously the attractive five-dimensional model where bulk fermions propagate along the $\mathcal{S}^1/\mathbb{Z}_2$ orbifold and interact with a Higgs boson localized at a fixed point of the extra dimension. The analytical calculation of the fermion mass spectrum and effective Yukawa couplings is shown to require the introduction of either essential boundary conditions (EBC) imposed by the model definition or certain bilinear brane terms (BBT) in the action, instead of the usual brane-Higgs regularizations. The obtained fermion profiles along the extra dimension turn out to undergo some discontinuities, in particular at the Higgs brane, which can be mathematically consistent if the action is well written with improper integrals. We also show that the $\mathbb{Z}_2$ parity transformations in the bulk do not affect the fermion chiralities, masses and couplings, in contrast with the EBC and the BBT, but when extended to the fixed points, they can generate the chiral nature of the theory and even select the Standard Model chirality setup while fixing as well the fermion masses and couplings. Thanks to the strict analysis developed, the duality with the interval model is scrutinized.

DOI: 10.1103/PhysRevD.103.075010

I. INTRODUCTION

As it is well known since the 2000s, the paradigm of models with additional spatial dimensions[1] constitutes an attractive alternative to supersymmetry for addressing the Standard Model (SM) puzzle of the gauge *hierarchy*. Furthermore, the warped dimension framework [1] with SM fermions in the whole bulk [2] offers an elegant geometrical principle of fermion profile overlap generating the SM fermion mass *hierarchy* [3] (see concrete application models, e.g., in Refs. [4–9]). In order to realize these two hierarchical features, the Brout-Englert-Higgs scalar field [10,11], which is at the origin of the SM particle masses through the electroweak symmetry breaking, must be stuck at the so-called TeV-brane[2] (or located in the bulk with a wave function strongly peaked at this brane). The TeV-brane is a 3-brane (three spatial dimensions) possibly at a boundary of the finite warped extra dimension.[3] More generally, a brane is an hypersurface located in an higher-dimensional space. It can arise in the context of string theories as D-branes which are dynamical objects with quantum properties [28,29] (see also Refs. [30,31] for the supergravity limit of string theories).[4]

In this paper, we will study the original version [1] of the warped dimension scenario based on the $\mathcal{S}^1/\mathbb{Z}_2$ orbifold [34,35] where the extra space is compactified on a circle respecting a spatial parity of the Lagrangian.[5] Focusing our attention on the subtle bulk fermion interactions with the brane-Higgs field localized at a fixed point, we will analyze the toy model with a flat extra dimension and the minimal field content: the results obtained on the fermion-Higgs coupling structure are directly applicable to the realistic warped model.

We will clarify the treatment of the bulk fermion couplings to the brane-localized Higgs boson, within the $\mathcal{S}^1/\mathbb{Z}_2$ orbifold background, by building rigorously the four-dimensional (4D)[6] effective Lagrangian of the minimal model, that is by calculating consistently the

[*]ruifeng.leng@ijclab.in2p3.fr
[†]moreau@ijclab.in2p3.fr
[‡]nortier@ijclab.in2p3.fr

[1]Together with the composite Higgs models which are dual models via the AdS/CFT correspondance.

[2]Let us mention here other possible phenomenological motivations, as from neutrino mass models, for the Higgs boson to be stuck at the boundary of an interval [12–16] or for fermions to propagate in the bulk [17,18].

[3]See for instance Ref. [19–26] for its phenomenology and Ref. [27] in a supersymmetric context.

[4]See Ref. [32,33] for brane-world effective field theories.

[5]An orbifold $\mathcal{O}$ being defined as an extra compact manifold $\mathcal{C}$ with so-called fixed points where the introduced spatial transformation (element from a discrete group G)—letting the Lagrangian invariant—is just equivalent to the identity. It is noted $\mathcal{O} = \mathcal{C}/G$ and possesses thus singularities, not like a smooth manifold [36,37].

[6]Including time.

Kaluza-Klein (KK) tower spectrum of fermion mass eigenvalues and the 4D effective Yukawa couplings (via the fermion wave functions along the extra dimension).

In particular, we will demonstrate that no brane-Higgs regularization [like smoothing the Higgs Dirac peak] should be applied (not necessary and no theoretical argument for it) in contrast with the usual regularization procedure of literature (see Ref. [38] and references therein) and that, instead, one must introduce either essential boundary conditions (EBC) on 5D fields,[7] originating from the $\mathbb{Z}_2$ symmetry, or equivalently some bilinear brane terms (BBT) in the fundamental 5D Lagrangian. The exact matching of the fermion mass spectra derived respectively through 4D and 5D methods will be used in order to confirm our analytical results. All those statements (except the 4D approach) hold as well for the free case, i.e., without Yukawa interactions.

This necessity of the presence of EBC or BBT (terms with the same form as in Refs. [38,39]), in the 4D or 5D approach, has been found as well [38] in the finite interval scenario (the higher-dimensional framework of the other warped model version) with identical brane-Higgs couplings to bulk fermions: this conclusion confirms that a specific treatment is required for pointlike interactions between bulk fermions and brane-Higgs bosons in higher-dimensional spaces.

Besides, we will strictly describe and work out the entire known duality: identical physical quantities, namely the mass eigenvalues and 4D effective Yukawa couplings, are obtained in the different $\mathcal{S}^1/\mathbb{Z}_2$ orbifold scenario with the Higgs boson localized at a fixed point and finite interval geometrical setup with the Higgs field stuck at a boundary.

The EBC and BBT (forms including signs) choices, which should originate from an Ultra-Violet (UV) completion of the theory, turn out to induce the chiral nature of the low-energy effective theory as well as realising the specific SM fermion chiralities. Indeed, all these chirality properties are in fact not selected by the remaining sign choices for the 5D fields transformed via the spatial $\mathbb{Z}_2$ group—as the solutions we find within this orbifold configuration can exhibit twist transformations (sign modification here) of the 5D fields, *à la* Scherk-Schwarz [40,41], through the extra space reflection. We will even show that the transformation sign choices are just mathematical conventions without physical impacts on the SM field chiralities, the fermion mass spectrum and the 4D effective Yukawa couplings.

Nevertheless, in order to clarify the chirality aspects, we will also study a different scenario—considered for example in Ref. [42]—where the $\mathbb{Z}_2$ transformation definitions on the fields cover as well the fixed points themselves.
It turns out that the associated transformation sign choices precisely at these fixed points constitute here additional EBC, noted EBC', that have the capacity to select some of the previous EBC and hence to fix the chirality setup. Once more, the role of these EBC' can be played instead by certain of the above BBT. Interestingly, such an inclusive $\mathbb{Z}_2$ symmetry definition can induce by itself the chiral nature of the theory as well as the SM chirality distribution over the various fields. This origin for the whole chirality configuration is not offered within the simpler interval model for instance. In the presence of brane-localized Yukawa couplings, such an inclusive $\mathbb{Z}_2$ scenario can only be treated through the 4D method. The fermion masses and couplings are also affected by this inclusive $\mathbb{Z}_2$ symmetry.

The action integral definition and integral domain endpoints will be treated carefully. In particular the decomposition of the action to introduce improper integrals will appear to be required in the presence of orbifold fixed points or pointlike fermion-boson interactions (not located at the boundary of a finite extra space like an interval). Within this new and appropriate approach of the specific points along the extra dimension of the orbifold, we find for the free or Yukawa case that some of the obtained consistent solutions exhibit certain field jumps at these fixed points and localized-interaction point. This interesting result of the possible existence of consistent profile jumps stands against one's first intuition [43,44], but those jumps are only induced by sign flipping and not by pointlike changes of the absolute value of the wave function amplitudes.

The analysis of the present orbifold background with brane-localized fermion-scalar interactions, as well as the previous results [38] on the interval background, show that generally speaking the action expression does not systematically contain all the information allowing to fully define the model: in particular some EBC may be used (in contrast, the BBT are terms in the action) depending on the brane treatment adopted or on the UV completion of the theory (which could introduce the BBT).

II. MINIMAL $\mathcal{S}^1/\mathbb{Z}_2$ CONSISTENT MODEL

A. Geometry and symmetries: the proper action

We consider the 5D space-time model with the product geometry $\mathcal{M}^4 \times \mathcal{S}^1/\mathbb{Z}_2$ described just below.

(i) $\mathcal{M}^4$ represents the usual 4D Minkowski space-time whose coordinates are denoted by x^μ where $\mu \in [\![0,3]\!]$ is the Lorentz index of the covariant formalism. The metric conventions are given in Appendix A.

[7] Directly imposed by the model definition, in contrast with the natural boundary conditions (NBC) deduced from the action minimization condition.

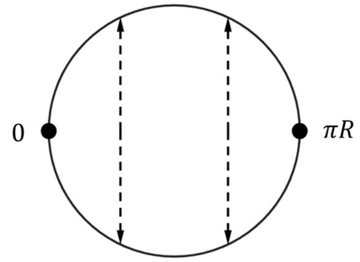

FIG. 1. $\mathcal{S}^1/\mathbb{Z}_2$ orbifold picture. The fixed points at $y=0$ and $y=\pi R$ are indicated by the two black points. The two examples of pairs of points with opposite coordinates, respectively indicated by the double dashed arrows, correspond to an identical Lagrangian density (for each pair).

(ii) $\mathcal{S}^1/\mathbb{Z}_2$ stands for the extra space orbifold obtained from modding out the circle $\mathcal{S}^1$ by the discrete group[8] symmetry $\mathbb{Z}_2$.

This circle $\mathcal{S}^1$ is characterized by a radius R and its coordinate is $y \in (-\pi R, \pi R]$, not double-counting the point $y=\pi R$ since it is this point, by pure convention, that is chosen to be the junction point geometrically identified with the point $y=-\pi R$ (which we note: $-\pi R \equiv \pi R$)[9] in order to implement the circle periodicity. The circle could be constructed from the real axis by imposing a periodicity, that is by identifying geometrically an infinite number of translated regions of size $2\pi R$ and hence by limiting the 1D space to the fundamental domain $(-\pi R, \pi R]$.

The (non-neutral) $\mathbb{Z}_2$ transformation on space, $y \to -y$,[10] has a representation on a generic 5D field,

$$\Phi(x^\mu, -y) = \mathcal{T}\Phi(x^\mu, y), \quad \forall\, y \in (-\pi R, 0) \cup (0, \pi R), \tag{2.1}$$

which must let the Lagrangian density invariant, by definition of the symmetry:

$$\mathcal{L}[\Phi(x^\mu, -y)] = \mathcal{L}[\Phi(x^\mu, y)], \quad \forall\, y \in (-\pi R, \pi R]. \tag{2.2}$$

We mention that this equation can define a class of equivalence of a given coordinate y_0, defined as $[y_0] = \{y \in \mathcal{S}^1 | y \sim y_0\}$ with $y \sim \pm y$, as illustrated symbolically on Fig. 1.

Two fixed points arise: $(y=0) \to (-0=0)$ and $(y=\pi R) \to (-\pi R \equiv \pi R)$. At these fixed points, the Lagrangian condition of Eq. (2.2) is automatically satisfied: $\mathcal{L}[\Phi(x^\mu, -0)] = \mathcal{L}[\Phi(x^\mu, 0)]$, and, $\mathcal{L}[\Phi(x^\mu, -\pi R)] = \mathcal{L}[\Phi(x^\mu, \pi R)]$, so that $\mathcal{T}$ is naturally taken as the identity operator in Eq. (2.1) since no transformation needs to apply on the fields there. Another scenario will be analysed in Sec. VI.

In order to properly write down the initial action, we urge the importance of taking care of possible field jumps along the extra dimension upon the reader. We are going to show that the existence of a field jump in field theory can make sense mathematically if the action integration domain is properly divided at the jump location. Different discontinuity configurations must be considered. First, the hypothesis of a possible jump at any point of the bulk would lead to an infinite number of cuts in the action integration region which would obviously not be treatable leading to unpredictable observables: this assumption is thus excluded. Second, assuming an arbitrary finite number of possible jumps and hence of mathematical separations in the action domain, outside the fixed points, is not expected to affect the unique physical results—like the fermion mass spectrum—since none of those jump points exhibit some specific property: it is thus useless to explore this direction. Third, the case of possible profile jumps at the two specific points that are the fixed points of the orbifold—one of those two, $y=\pi R$, corresponding as well to the Yukawa coupling location (see Sec. II B 3)—remains to be studied. The effective presence of such profile jumps in some of the obtained solutions (see Figs. 2 and 3 respectively for the free and coupled fermion situations) confirms this possibility. For example, in case of a profile jump at $y=0$ (an identical discussion holds for the other fixed point at $y=\pi R$), regarding a well-defined Lagrangian integrand involving 5D fields over the whole action integration domain, we simply have to choose between the mathematical definitions of the left or right continuity for a generic profile function along the extra dimension: $f(0) = f(0^-) = \lim_{\epsilon\to 0} f(0-\epsilon)$ with $\epsilon > 0$, or, $f(0) = f(0^+)$. This choice is conventional and hence cannot affect numerical results, so let us choose conveniently

$$f(0) = f(0^+) \quad \text{and} \quad f(\pi R^-) = f(\pi R) \tag{2.3}$$

throughout this paper, in case of jumps at the fixed points. Then, the well-defined global action of this model must be written as a sum of some brane terms, an improper integral and a standard integration over different regions covering the whole physical domain of the circle:

[8] Factor element, $e^{\pm i\frac{2\pi}{2}} = -1$, and neutral element, 1.

[9] Another possible mathematical convention would have been, for instance, $-\frac{3\pi R}{2} \equiv \frac{\pi R}{2}$.

[10] The convention above, of having taken the coordinate origin at the strict middle of the circle domain (or fundamental domain), renders the $\mathbb{Z}_2$ parity with respect to the origin more explicit and convenient to study.

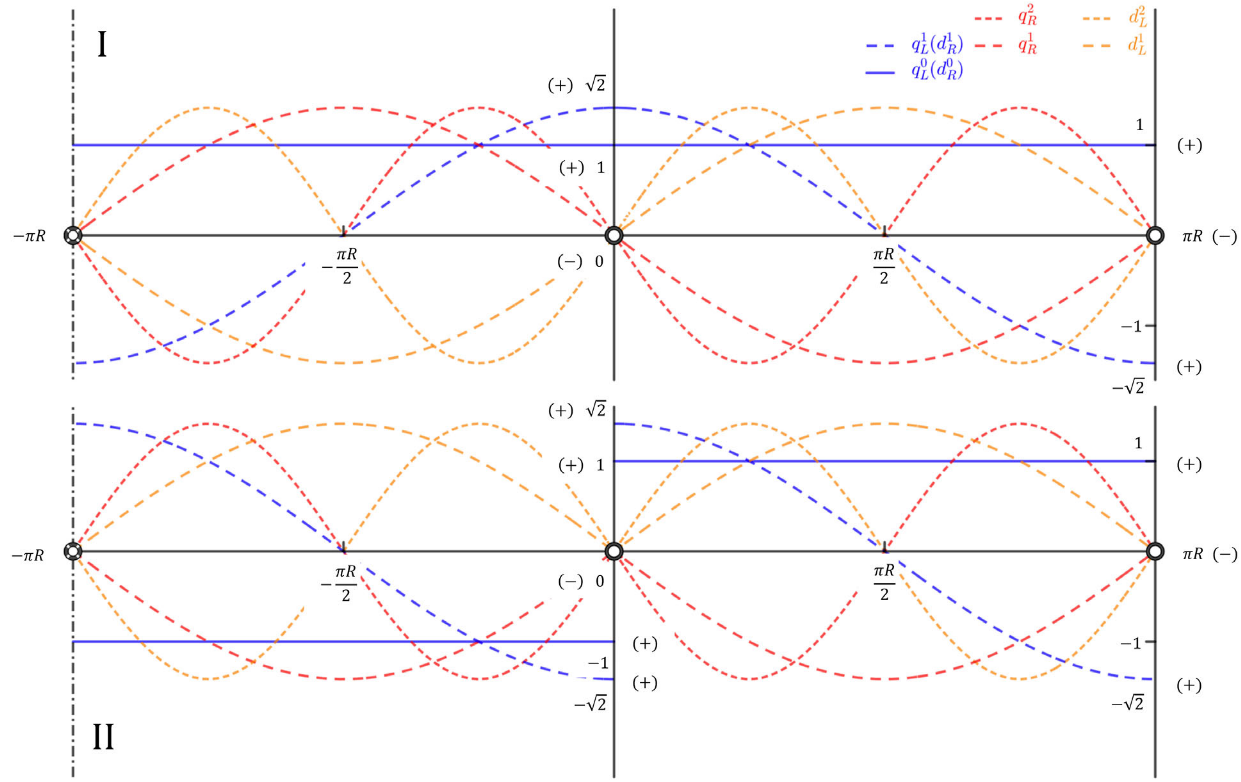

FIG. 2. Zero-mode and KK dimensionless wave functions $q^n_{L/R}(y)$, $d^n_{L/R}(y)$, with $n = 0$, 1, 2, along the $\mathcal{S}^1/\mathbb{Z}_2$ orbifold domain, $y \in [-\pi R^+, 0^-] \cup [0, \pi R]$, corresponding to the free solutions of Table I in the simplified case, $\alpha^n_{Q,D} = 0$, $m_n > 0$, and for the two different types of $\mathbb{Z}_2$ transformations, *I*, *II* from Eqs. (3.8) and (3.9). The two fixed points at, $y = 0$, $y = \pi R \equiv -\pi R$, and Dirichlet/Neumann BC, $(-)/(+)$, are indicated on the graph.

$$S_{5\mathrm{D}} = S_{\mathrm{bulk}} + S_{\mathrm{branes}}, \quad \text{with,} \quad S_{\mathrm{bulk}} = \int d^4x \left(\int_{-\pi R^+}^{0^-} dy \mathcal{L}_{\mathrm{kin}} + \int_0^{\pi R} dy \mathcal{L}_{\mathrm{kin}} \right), \quad \text{and,}$$
$$\int d^4x \int_{-\pi R^+}^{0^-} dy \mathcal{L}_{\mathrm{kin}} \hat{=} \lim_{a\to 0^-, b\to -\pi R^+} \int d^4x \int_b^a dy \mathcal{L}_{\mathrm{kin}} = \lim_{\epsilon\to 0} \int d^4x \int_{-\pi R+\epsilon}^{0-\epsilon} dy \mathcal{L}_{\mathrm{kin}}, \tag{2.4}$$

where $\epsilon > 0$, S_{branes} represents action terms located at the orbifold fixed points and $\mathcal{L}_{\mathrm{kin}}$ stands for the fermion kinetic terms of the Lagrangian density (see next subsection). Indeed, all the obtained fields will be well defined at the two fixed points via Eq. (2.3). Besides, for $\mathcal{L}_{\mathrm{kin}}$ to be integrable over the entire region $y \in [0, \pi R]$, this Lagrangian density, which will involve profile derivatives $f'(y)$, must be well-defined over this region. The necessary (but not sufficient) condition for this last feature is that the profiles $f(y)$ have to be continuous on $[0, \pi R]$ and Eq. (2.3) also guarantees this continuity. For the consistency of the other integration term in Eq. (2.4), the profile continuity along $y \in [-\pi R^+, 0^-]$[11] obviously reads as:

$$\lim_{\kappa\to 0} f(0^- - \kappa) = \lim_{\epsilon\to 0}\lim_{\kappa\to 0} f([0-\epsilon] - \kappa)$$
$$= \lim_{\omega\to 0} f(0-\omega) = f(0^-),$$

with $\kappa > 0$, $\epsilon > 0$, $\omega = \epsilon + \kappa$ and similar equalities hold at the other region boundary $y = -\pi R^+$. Furthermore, the worked out solutions $f(y)$ will (well) be derivable over the two regions $[-\pi R^+, 0^-]$ and $[0, \pi R]$ (see Secs. III B and V C respectively for the free and coupled fermion situations) so that $\mathcal{L}_{\mathrm{kin}}$ will be well defined. For example, $f(y)$ is derivable in the region $[0, \pi R]$ at $y = 0$ if and only if $f(y)$ is right-derivable at $y = 0$, and the corresponding right-derivative does not diverge thanks to the first equality of Eq. (2.3). Notice that from the point of view of the integration by pieces of the action in Eq. (2.4) precisely over the physical domain, the inclusion (or not) of the single points at $y = 0$ or $y = \pi R \equiv -\pi R$ does not affect the integral results—given the continuous form of the even $\mathcal{L}_{\mathrm{kin}}$ over

[11]To be clear, the integration domain $[-\pi R^+, 0^-]$ corresponds to the spatial region along the extra dimension $]-\pi R, 0[\Leftrightarrow (-\pi R, 0)$—respectively the Francophone and Anglophone notations—which does not include the fixed points at $y = 0$ and $y = -\pi R$.

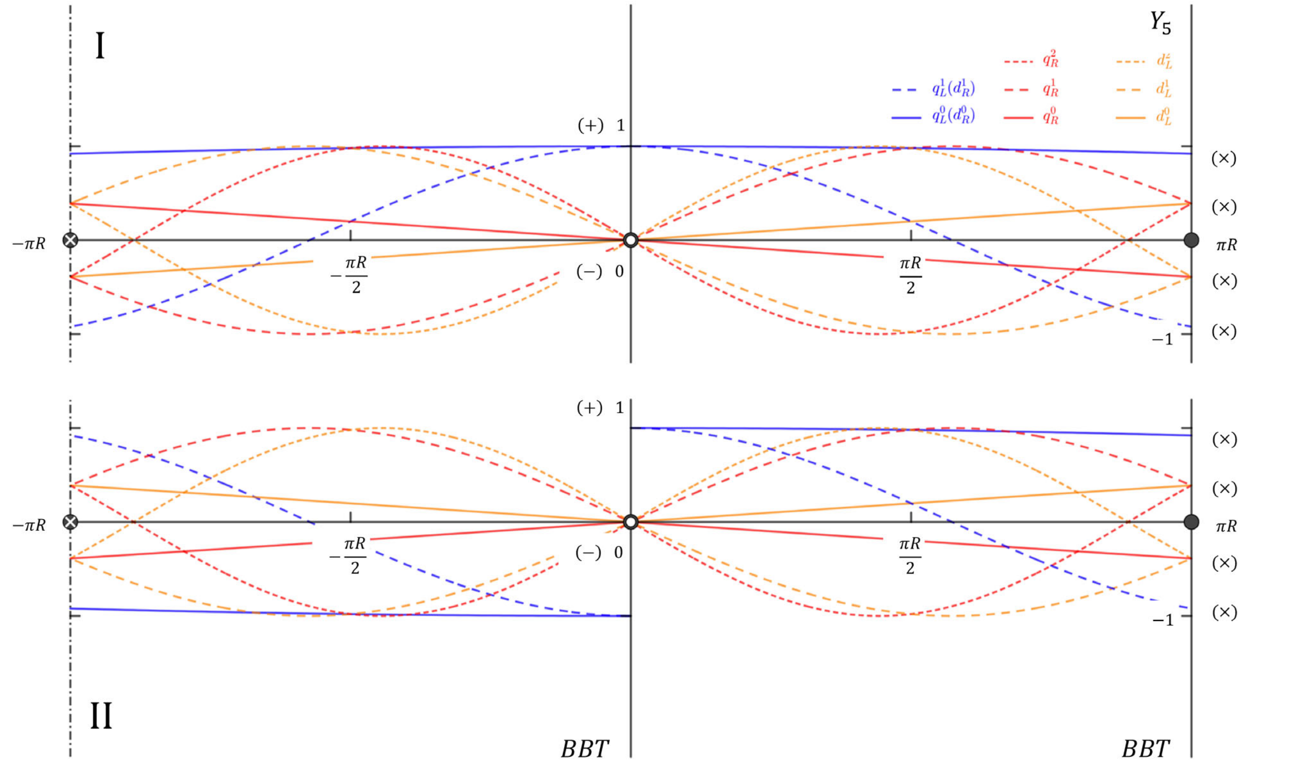

FIG. 3. Zero-mode and excitation wave functions $q^n_{L/R}(y)$, $d^n_{L/R}(y)$, with $n = 0$, 1, 2, along the $\mathcal{S}^1/\mathbb{Z}_2$ orbifold domain, $y \in [-\pi R^+, 0^-] \cup [0, \pi R]$, corresponding to the Yukawa-coupled solutions (5.18), presented in Table II, for the simplified case, $\alpha_Y = \alpha^n_0 = 0$, and the two different types of $\mathbb{Z}_2$ transformations, *I*, *II* from Eqs. (5.7)–(3.9). The two fixed points at, $y = 0$, $y = \pi R \equiv -\pi R$, the BC, $(-)/(+)/(\times)$, the BBT and Yukawa coupling brane-locations are indicated on the graph.

the two regions—so that only consistent action definition arguments were considered here.

Finally, the Lagrangians of the whole expression (2.4) will respect the $\mathbb{Z}_2$ symmetry since the Lagrangian $\mathcal{L}_{\rm kin}$ will fulfill the condition (2.2) and the brane action will exclusively involve Lagrangians taken at fixed points like for example [see Eq. (2.13)], $S_{\rm branes} \ni S_Y = \int d^4x \mathcal{L}_Y(x^\mu, \pi R)$.

B. Field content and complete action

1. Bulk fermion fields

Let us introduce the minimal spin-1/2 field content which allows to write down a SM Yukawa-like coupling between zero mode fermions (of different chiralities) and a spin-0 field (see Sec. II B 3). It is constituted by a pair of fermion fields called Q and D. Those particles propagate along the circle $\mathcal{S}^1$, as we have in mind an extension of this toy model to a realistic scenario with bulk matter (cf., Sec. II B 4) where Q, D will represent respectively the $\mathrm{SU}(2)_L$ gauge doublet down-component quark and the singlet down-quark.

The 5D fields $Q(x^\mu, y)$ and $D(x^\mu, y)$—of mass dimension 2—have the following kinetic terms [entering Eq. (2.4)] which allow to recover canonical covariant kinetic terms for the associated fermions in the 4D effective action (as imposed by the argument of decoupling limit[12]):

$$\mathcal{L}_{\rm kin} = \frac{i}{2}(\bar{Q}\Gamma^M \overleftrightarrow{\partial}_M Q + \bar{D}\Gamma^M \overleftrightarrow{\partial}_M D), \tag{2.5}$$

using the standard notations $\overleftrightarrow{\partial}_M = \vec{\partial}_M - \overleftarrow{\partial}_M$, $\partial_M = \partial/\partial x^M$, $x^M = (x^\mu, y)$ with $M \in [\![0, 4]\!]$ for the coordinates $x^M \in \mathcal{M}^4 \times \mathcal{S}^1/\mathbb{Z}_2$ and Γ^M for the 5D Dirac matrices (cf., Appendix A). In the used conventions, the 5D Dirac spinor, being in the irreducible representation of the Lorentz group, reads for example for Q as,

$$Q = \mathcal{Q}_L + \mathcal{Q}_R \quad \text{with} \quad \mathcal{Q}_L = \begin{pmatrix} Q_L \\ 0 \end{pmatrix}, \quad \mathcal{Q}_R = \begin{pmatrix} 0 \\ Q_R \end{pmatrix}, \tag{2.6}$$

in terms of the two two-component Weyl spinors Q_L, Q_R, L/R standing for the left/right chirality, and as usually $\bar{Q} = Q^\dagger \gamma^0$.

[12]From the theoretical consistency and phenomenological points of view, the SM must be approximately recovered at low-energies in the limit of infinitely heavy KK excitations.

As stated at the end of previous section, the Lagrangian $\mathcal{L}_{\rm kin}$ must obey the condition (2.2). For this purpose, the $\mathbb{Z}_2$ transformation (2.1) on the 5D fields $Q(x^\mu, y)$ and $D(x^\mu, y)$ can take four different forms which constitute essential conditions (EC) issued from the model definition:

$$\text{Type I}\begin{cases} Q(x^\mu,-y) = -\gamma^5 Q(x^\mu,y) \Rightarrow Q_L \text{ even}, & Q_R \text{ odd}, \\ D(x^\mu,-y) = \gamma^5 D(x^\mu,y) \Rightarrow D_L \text{ odd}, & D_R \text{ even}, \end{cases} \tag{2.7}$$

$$\text{Type II}\begin{cases} Q(x^\mu,-y) = \gamma^5 Q(x^\mu,y) \Rightarrow Q_L \text{ odd}, & Q_R \text{ even}, \\ D(x^\mu,-y) = -\gamma^5 D(x^\mu,y) \Rightarrow D_L \text{ even}, & D_R \text{ odd}, \end{cases} \tag{2.8}$$

$$\text{Type III}\begin{cases} Q(x^\mu,-y) = -\gamma^5 Q(x^\mu,y) \Rightarrow Q_L \text{ even}, & Q_R \text{ odd}, \\ D(x^\mu,-y) = -\gamma^5 D(x^\mu,y) \Rightarrow D_L \text{ even}, & D_R \text{ odd}, \end{cases} \tag{2.9}$$

$$\text{Type IV}\begin{cases} Q(x^\mu,-y) = \gamma^5 Q(x^\mu,y) \Rightarrow Q_L \text{ odd}, & Q_R \text{ even}, \\ D(x^\mu,-y) = \gamma^5 D(x^\mu,y) \Rightarrow D_L \text{ odd}, & D_R \text{ even}, \end{cases} \tag{2.10}$$

under which the Lagrangian (2.5) is indeed invariant, as appears by using the properties of the γ_5 Dirac matrix and the odd parity of the fifth partial derivative ∂_4. Notice that the $\mathbb{Z}_2$ parity (second order cyclic group) does not allow complex phase factors in the transformations:

$$F|_y = e^{i\theta_F}\gamma^5 F|_{-y} = e^{i\theta_F}\gamma^5 e^{i\theta_F}\gamma^5 F|_y = (e^{i\theta_F})^2 F|_y.$$

Using the γ_5 definition of Appendix A together with Eq. (2.6), we already deduce some information on the possible 5D chiral field parities with respect to $y = 0$, as indicated in Eqs. (2.7)–(2.10).

Based on Eq. (2.6), we can rewrite the bulk Lagrangian of Eq. (2.5) in forms which are convenient to see at a glance the Lagrangian even parity, simply by using the occurrence of fixed 5D field parities, different for the left/right chiralities [cf., Eqs. (2.7)–(2.10)], and the ∂_4 odd parity:

$$\begin{aligned}\mathcal{L}_{\rm kin} &= \frac{1}{2}(iQ_R^\dagger \sigma^\mu \overleftrightarrow{\partial_\mu} Q_R + iQ_L^\dagger \bar{\sigma}^\mu \overleftrightarrow{\partial_\mu} Q_L - Q_R^\dagger \overleftrightarrow{\partial_4} Q_L \\ &\quad + Q_L^\dagger \overleftrightarrow{\partial_4} Q_R) + \{Q \leftrightarrow D\}, \\ &= \frac{1}{2}(i\bar{\mathcal{Q}}_R \gamma^\mu \overleftrightarrow{\partial_\mu} \mathcal{Q}_R + i\bar{\mathcal{Q}}_L \gamma^\mu \overleftrightarrow{\partial_\mu} \mathcal{Q}_L - \bar{\mathcal{Q}}_R \overleftrightarrow{\partial_4} \mathcal{Q}_L \\ &\quad + \bar{\mathcal{Q}}_L \overleftrightarrow{\partial_4} \mathcal{Q}_R) + \{\mathcal{Q} \leftrightarrow \mathcal{D}\},\end{aligned}$$

where the low double arrows indicate a replacement of 5D fields in the previous terms and the matrices $\sigma^\mu, \bar{\sigma}^\mu$ are defined in Appendix A.

2. Brane-localized scalar field

The questions about the mass calculation arise when the bulk fermions couple to a single 4D real scalar field H (mass dimension 1) which is confined at a fixed point of the orbifold, as in the studied model (inspired by the warped scenario addressing the gauge hierarchy problem). We simply choose this fixed point to be at $y = \pi R$, rather than $y = 0$, which is a purely mathematical convention since these two points belong to a circle. The real scalar field has an action of the generic form,

$$S_H = \int d^4x \left[\frac{1}{2}\partial_\mu H \partial^\mu H - V(H)\right], \tag{2.11}$$

with a potential V possessing a minimum which generates a nonvanishing vacuum expectation value (VEV) for the field H expanded as

$$H(x^\mu) = \frac{v + h(x^\mu)}{\sqrt{2}}, \tag{2.12}$$

in analogy with the SM Higgs field.

3. Yukawa interactions

We consider the following Yukawa interactions allowing to study the subtleties induced by the coupling of the above brane-scalar field (at $y = \pi R$) to the introduced bulk fermions,

$$\begin{aligned} S_Y &= \int d^4x \mathcal{L}_Y(x^\mu, \pi R), \quad \text{with}, \\ \mathcal{L}_Y &= -Y_5 H Q_L^\dagger D_R - Y_5' H Q_R^\dagger D_L + \text{H.c.}. \end{aligned} \tag{2.13}$$

Notice that considering operators involving the fields H, Q, D up to dimension 5 allows to include such a Yukawa coupling. Let us recall here that in case of profile jumps at the fixed point at $y = \pi R$, the 5D fields $Q_{L/R}(x^\mu, \pi R)$, $D_{L/R}(x^\mu, \pi R)$ are defined through the profile convention (2.3), as already described. The studied model with a Yukawa coupling at a fixed point will turn out to be dual to the interval model including a Yukawa coupling at a boundary (see Sec. VII).

The complex $Y_5 = \mathrm{e}^{i\alpha_Y}|Y_5|$ and $Y_5' = \mathrm{e}^{i\alpha_Y'}|Y_5'|$ Yukawa coupling constants, entering Eq. (2.13), are independent and a well-defined 4D chirality holds for the fermion fields on the 3-brane strictly at $y = \pi R$ [38,44]. To avoid the introduction of a new energy scale, in the spirit of the warped model, we can define the 5D Yukawa coupling constants as

$$Y_5 = y_4 \times 2\pi R, \quad \text{and}, \quad Y_5' = y_4' \times 2\pi R, \tag{2.14}$$

where y_4, y_4' are dimensionless coupling constants of $\mathcal{O}(1)$. Then, y_4 can be approximately identified with the SM

TABLE I. SM-like free fermionic $f^n_{L/R}(y)$ profiles—normalized to the indicated complex phases—on the two orbifold domains $[-\pi R^+, 0^-]$ and $[0, \pi R]$, corresponding to the solution of line 1 (2) in Eq. (3.18) for the field D (Q). The associated mass spectrum (3.20) is included as well for completeness. The profiles are given for the four types of $\mathbb{Z}_2$ transformations (3.8)–(3.9). The phases $\alpha^n_{Q/D}$ belong to $\mathbb{R}$. In the special case, $n = 0$, the $\sqrt{2}$ factors must all be replaced by the unity.

		Fields			
		$Q_{L/R}$		$D_{L/R}$	
Continuity domains	$\mathbb{Z}_2$	$q^n_L(y)/e^{i\alpha^n_Q}$	$q^n_R(y)/e^{i\alpha^n_Q}$	$d^n_L(y)/e^{i\alpha^n_D}$	$d^n_R(y)/e^{i\alpha^n_D}$
$[0, \pi R]$	Any	$\sqrt{2}\cos(m_n y)$	$-\sqrt{2}\sin(m_n y)$	$\sqrt{2}\sin(m_n y)$	$\sqrt{2}\cos(m_n y)$
$[-\pi R^+, 0^-]$	I	$\sqrt{2}\cos(m_n y)$	$-\sqrt{2}\sin(m_n y)$	$\sqrt{2}\sin(m_n y)$	$\sqrt{2}\cos(m_n y)$
	II	$-\sqrt{2}\cos(m_n y)$	$\sqrt{2}\sin(m_n y)$	$-\sqrt{2}\sin(m_n y)$	$-\sqrt{2}\cos(m_n y)$
	III	$\sqrt{2}\cos(m_n y)$	$-\sqrt{2}\sin(m_n y)$	$-\sqrt{2}\sin(m_n y)$	$-\sqrt{2}\cos(m_n y)$
	IV	$-\sqrt{2}\cos(m_n y)$	$\sqrt{2}\sin(m_n y)$	$\sqrt{2}\sin(m_n y)$	$\sqrt{2}\cos(m_n y)$
KK Masses		$\lvert m_n\rvert = n/R,\ n \in \mathbb{N}$			

Yukawa coupling constant within the decoupling limit, as will be described in Eqs. (5.22) and (5.23).

When calculating the tower of excited fermion masses, we restrict our considerations to the VEV of H and concentrate our attention on the following part of the action (2.13),

$$S_X = \int d^4x \mathcal{L}_X(x^\mu, \pi R), \quad \text{with,}$$
$$\mathcal{L}_X = -X Q_L^\dagger D_R - X' Q_R^\dagger D_L + \text{H.c.}, \tag{2.15}$$

with the compact notations $X = vY_5/\sqrt{2}$ and $X' = vY'_5/\sqrt{2}$. Based on Eq. (2.12), the complete action reads as, $S_Y = S_X + S_{\text{int}}$, with the localized fermion-scalar interaction terms:

$$S_{\text{int}} = \int d^4x \mathcal{L}_{\text{int}}(x^\mu, \pi R), \quad \text{with,}$$
$$\mathcal{L}_{\text{int}} = -\frac{Y_5}{\sqrt{2}} h Q_L^\dagger D_R - \frac{Y'_5}{\sqrt{2}} h Q_R^\dagger D_L + \text{H.c.}, \tag{2.16}$$

that allow to work out the 4D effective Yukawa coupling constants.

4. Bilinear brane terms

Introducing all the covariant operators up to mass dimension 5 [like for the Yukawa couplings (2.13)] in this model, one should consider as well the dimension 4 operators given just below, that we call the BBT like in Ref. [38]. Furthermore, the presence of the BBT has several justifications: (i) they allow to avoid physical consistency problems both in the free case (see Secs. III A and III C) and with Yukawa couplings (Secs. V A and V C); (ii) they play the role of defining well the model at the two orbifold fixed points both in the free case (see Secs. III B and III C) and with Yukawa couplings (Sec. V C); (iii) they induce the expected matching of the analytical results on the spectrum derived through the 4D and 5D approaches (see Secs. IV and V C).

The following BBT lead to the SM chirality configuration,

$$S_B = \int d^4x (\sigma_0^Q \bar{Q}Q|_0 + \sigma_{\pi R}^Q \bar{Q}Q|_{\pi R} + \sigma_0^D \bar{D}D|_0 + \sigma_{\pi R}^D \bar{D}D|_{\pi R}), \tag{2.17}$$

where $\sigma^Q_{0(\pi R)} = \underset{(-)}{+}$, $\sigma^D_{0(\pi R)} = \underset{-}{(+)}$ and for example $\bar{Q}Q|_0 = \bar{Q}(x^\mu, 0) Q(x^\mu, 0)$. Indeed, without Yukawa couplings, these terms will induce only a nonvanishing profile $q^0_L(y)$ [see line 2 of Eq. (3.18) and Table I in case of the zero-mode with mass $m_0 = 0$] in the 5D field $Q_L(x^\mu, y)$ so that only the left-handed 4D field $Q^0_L(x^\mu)$ will exist. This zero-mode $Q^0_L(x^\mu)$, without KK mass contribution, constitutes the lightest mode of the KK tower and also the SM state. Hence, we can well recover the SM configuration: a chiral field content and a left-handed 4D field potentially representing the $\mathrm{SU}(2)_\mathrm{L}$ quark doublet in the direct extension to gauge symmetries (and three flavors). Given that, similarly, the BBT (2.17) will exclusively lead to a right-handed 4D field $D^0_R(x^\mu)$ [line 1 of Eq. (3.18)] potentially representing the SM down quark type (gauge singlet). When adding the Yukawa couplings (2.13), this SM chirality set-up remains though it is no more explicit due to the $Q^n(x^\mu) - D^n(x^\mu)$ mixing, via vector-like KK state mixings, which induces some vector-like mass eigenstates $\psi^0_{L/R}(x^\mu)$ for the lightest modes of the tower (see Secs. IV and V C). In the decoupling limit where heavy KK state mixings tend to vanish, the SM chirality configuration is recovered as expected.

For completeness, let us underline that in the free case, the opposite BBT signs, $\sigma^Q_{0(\pi R)} = \underset{-}{(+)}$, $\sigma^D_{0(\pi R)} = \underset{(-)}{+}$, would lead to a chiral set-up for the zero-modes but different from the potential SM chirality configuration, namely: $Q^0_R(x^\mu)$, $D^0_L(x^\mu)$. Similarly, the BBT signs, $\sigma^Q_{0(\pi R)} = \underset{(-)}{+}$, $\sigma^D_{0(\pi R)} = \underset{(-)}{+}$, would lead to the setup, $Q^0_L(x^\mu)$, $D^0_L(x^\mu)$, and $\sigma^Q_{0(\pi R)} = \underset{-}{(+)}$, $\sigma^D_{0(\pi R)} = \underset{-}{(+)}$, to, $Q^0_R(x^\mu)$, $D^0_R(x^\mu)$.

Finally, as will be described in the Secs. III B and III C, the possible signs, $\sigma^Q_{0(\pi R)} = \pm$ (same sign for 0 and πR), would instead lead to the profile solutions (3.19) with two non-vanishing profiles for the lightest modes (as $m_0 \neq 0$) and hence to vectorlike states: $Q^0_{L/R}(x^\mu)$. The same statement holds for $\sigma^D_{0(\pi R)} = \pm$ and thus $D^0_{L/R}(x^\mu)$. Such massive vectorlike states[13] can be used to build custodially protected warped models [50] and are then called custodians (see for instance Ref. [9]). Of course there exist 8 remaining cases combining the above Lagrangian sign configurations: $\sigma^Q_{0(\pi R)} = \underset{(-)}{+}$, $\underset{-}{(+)}$, $\sigma^D_{0(\pi R)} = \pm$, and, $\sigma^Q_{0(\pi R)} = \pm$, $\sigma^D_{0(\pi R)} = \underset{(-)}{+}$, $\underset{-}{(+)}$.

Therefore, it appears clearly that the BBT control the chiral configurations of the model. The UV completion of the theory can be at the origin of the BBT and hence of the chirality setup: chiral nature of the theory and specific chiralities of the various fields.

To end up this section, we note that the complete toy model studied is characterized by the action,

$$S_{5D} = S_{\rm bulk} + S_{\rm branes} = S_{\rm bulk} + S_H + S_X + S_{\rm int} + S_B. \tag{2.18}$$

The conclusions that will be derived in the present work can be directly extended to the realistic warped model with SM bulk matter addressing the fermion mass and gauge hierarchies, along the same lines as the flavor and gauge symmetry generalizations described in details in the Sec. 2.6 of Ref. [38].

III. FREE BULK FERMIONS ON THE ORBIFOLD

In this section, we calculate the fermionic mass spectrum for the free case where $Y_5 = Y'_5 = 0$ in the action piece S_Y given by Eq. (2.13).

A. Applying the NBC

We start by considering the bulk action part,

$$S_{\rm bulk},$$

of Eq. (2.4), from the considered action, S_{5D}, of Eq. (2.18). We apply the least action principle to it which leads to two relations of the kind, $\delta_{\bar F} S_{\rm bulk} = 0$, one for each of the unknown 5D fields $F = Q,\, D$, and two corresponding ones, $\delta_F S_{\rm bulk} = 0$, involving the complex conjugate fields,[14] since the elementary field variations δQ_α, $\delta \bar Q_\alpha$, δD_α and $\delta \bar D_\alpha$ (see Appendix B 1) are generic and hence independent from each other. Using compact notations, like for example,

$$\sum_{\alpha=1}^{4} \delta \bar F_\alpha \frac{\partial \mathcal{L}_{\rm kin}}{\partial \bar F_\alpha} \doteq \delta \bar F \frac{\partial \mathcal{L}_{\rm kin}}{\partial \bar F},$$

we can write in particular,[15]

$$\begin{aligned}
\delta_{\bar F} S_{\rm bulk} &= \int d^4x \left(\int_{-\pi R^+}^{0^-} + \int_0^{\pi R} \right) dy \left\{ \delta \bar F \frac{\partial \mathcal{L}_{\rm kin}}{\partial \bar F} + \delta(\partial_M \bar F) \frac{\partial \mathcal{L}_{\rm kin}}{\partial \partial_M \bar F} \right\} \\
&= \int d^4x \left(\int_{-\pi R^+}^{0^-} + \int_0^{\pi R} \right) dy \left\{ \delta \bar F \frac{\partial \mathcal{L}_{\rm kin}}{\partial \bar F} + \partial_M \left[\delta \bar F \frac{\partial \mathcal{L}_{\rm kin}}{\partial \partial_M \bar F} \right] - \delta \bar F \partial_M \frac{\partial \mathcal{L}_{\rm kin}}{\partial \partial_M \bar F} \right\} \\
&= \int d^4x \left(\int_{-\pi R^+}^{0^-} + \int_0^{\pi R} \right) dy \left\{ \delta \bar F \left[\frac{\partial \mathcal{L}_{\rm kin}}{\partial \bar F} - \partial_M \frac{\partial \mathcal{L}_{\rm kin}}{\partial \partial_M \bar F} \right] \right\} \\
&\quad + \int d^4x \left(\delta \bar F \frac{\partial \mathcal{L}_{\rm kin}}{\partial \partial_4 \bar F} \bigg|_{-\pi R^+}^{0^-} + \delta \bar F \frac{\partial \mathcal{L}_{\rm kin}}{\partial \partial_4 \bar F} \bigg|_0^{\pi R} \right).
\end{aligned} \tag{3.1}$$

Based on the Lagrangian $\mathcal{L}_{\rm kin}$ of Eq. (2.5), these two bulk terms take the same form (the first one being calculated explicitly in Eq. (B6) to clarify the spinor component treatment) and the two remaining brane terms can be calculated as well:

[13] Extensive phenomenology at colliders has been developed about such vectorlike particles [45–49].

[14] The equations of motion and boundary conditions derived from the least action principle for the fields and their conjugates are trivially related through the Hermitian conjugation.

[15] We omit the global 4-divergence which vanishes in the action integration due to vanishing fields at the boundaries at infinities. Indeed, when minimizing the action, the varied terms must vanish separately at infinite boundaries, since the nonvanishing field variations at boundaries are independent from each other and from the bulk ones (see also Ref. [51]). This is realized by the local physics statement which induces vanishing fields at infinities due to the wave function normalization conditions (see also Ref. [52]).

$$\delta_{\bar{F}} S_{\text{bulk}} = \int d^4x \left(\int_{-\pi R^+}^{0^-} + \int_0^{\pi R} \right) dy \{ \delta\bar{F} [i\Gamma^M \partial_M F] \} + \int d^4x \left(\delta\bar{F} \left[-\frac{\gamma^5}{2} F \right] \Big|_{0^+}^{\pi R^-} + \delta\bar{F} \left[-\frac{\gamma^5}{2} F \right] \Big|_0^{\pi R} \right), \tag{3.2}$$

where we have further invoked the $\mathbb{Z}_2$ transformations (2.7)–(2.10) for the generic 5D field, Eq. (B7) for its variation and γ^5 properties:

$$\delta\bar{F} \left[-\frac{\gamma^5}{2} F \right] \Big|_{0^-, -\pi R^+} = (\mp \delta\bar{F}\gamma^5) \left[-\frac{\gamma^5}{2} (\pm \gamma^5 F) \right] \Big|_{0^+, \pi R^-} = -\delta\bar{F} \left[-\frac{\gamma^5}{2} F \right] \Big|_{0^+, \pi R^-}.$$

Then thanks to Eq. (2.3)[16] and Eqs. (B4) and (B5), respectively, the expression (3.2) simplifies to,

$$\begin{aligned} \delta_{\bar{F}} S_{\text{bulk}} &= \int d^4x \left(\int_{-\pi R^+}^{0^-} + \int_0^{\pi R} \right) dy \{ \delta\bar{F} [i\Gamma^M \partial_M F] \} + \int d^4x 2\delta\bar{F} \left[-\frac{\gamma^5}{2} F \right] \Big|_0^{\pi R} \\ &= \int d^4x \left(\int_{-\pi R^+}^{0^-} + \int_0^{\pi R} \right) dy \{ \delta\bar{F} [i\Gamma^M \partial_M F] \} + \int d^4x [\delta F_R^\dagger F_L - \delta F_L^\dagger F_R]|_0^{\pi R}. \end{aligned} \tag{3.3}$$

In this expression, the bulk and brane variations—respectively the volume and surface terms—must vanish separately due to independent field variations (no reason to be linked). Besides all those field variations are not vanishing (unknown fields) so that we get the bulk equations of motion (EOM),

$$i\Gamma^M \partial_M F = 0, \quad \forall\, x^\mu, \quad \forall\, y \in [-\pi R^+, 0^-] \cup [0, \pi R], \tag{3.4}$$

and the natural boundary conditions (NBC),

$$F_L|_0 = F_R|_0 = F_L|_{\pi R} = F_R|_{\pi R} = 0. \tag{3.5}$$

At this level, we can first solve Eq. (3.4) together with Eq. (3.5) to find out the F fields over the domain, $y \in [0, \pi R]$. This is precisely what has been done in the preliminary Ref. [38] where the two exactly identical Eqs. (3.3) and (3.4) [there] have been solved over the interval, $y \in [0, L]$. Since the fields are continuous over $y \in [0, \pi R]$ [cf., Eq. (2.3)] like there over $y \in [0, L]$, we can thus apply here the results obtained in this reference: the solutions found for Eqs. (3.4) and (3.5) are expressed through the KK decomposition (with a similar choice of global factor),

$$F_{L/R}(x^\mu, y) = \frac{1}{\sqrt{2\pi R}} \sum_{n=0}^{+\infty} f_{L/R}^n(y) F_{L/R}^n(x^\mu), \tag{3.6}$$

where the 4D fields $F_{L/R}^n = Q_{L/R}^n, D_{L/R}^n$ represent the KK states and satisfy the Dirac-Weyl equations,

$$\forall\, n \in \mathbb{N}, \begin{cases} i\bar{\sigma}^\mu \partial_\mu F_L^n(x^\mu) - m_n F_R^n(x^\mu) = 0, \\ i\sigma^\mu \partial_\mu F_R^n(x^\mu) - m_n F_L^n(x^\mu) = 0, \end{cases} \tag{3.7}$$

involving the KK mass eigenvalues m_n, while the only resulting profiles $f_{L/R}^n(y) = q_{L/R}^n(y), d_{L/R}^n(y)$, included respectively into $F = Q, D$, are vanishing over $y \in [0, \pi R]$. The opposite signs in front of each mass term of the bulk profile EOM induced by Eq. (3.4), with respect to the calculations of Ref. [38], just originate from a different sign convention for the Γ^4 matrix [see Eq. (A3)] and hence do not modify the (un)physical result of vanishing profiles. Now let us study the profile solutions in the complementary region, $y \in [-\pi R^+, 0^-]$. Inserting the KK decomposition (3.6) into the first type of $\mathbb{Z}_2$ transformation (2.7), one obtains the $\mathbb{Z}_2$ transformations directly on the $f_{L/R}^n(y)$ profiles ($\forall\, n \in \mathbb{N}$):

$$\text{Type I} \begin{cases} \sum_{n=0}^{+\infty} [q_{L(R)}^n(-y) \underset{-}{(+)} q_{L(R)}^n(y)] Q_{L(R)}^n(x^\mu) = 0 \Rightarrow q_{L(R)}^n(-y) = \underset{(-)}{+} q_{L(R)}^n(y) \\ \sum_{n=0}^{+\infty} [d_{L(R)}^n(-y) \underset{(-)}{+} d_{L(R)}^n(y)] D_{L(R)}^n(x^\mu) = 0 \Rightarrow d_{L(R)}^n(-y) = \underset{-}{(+)} d_{L(R)}^n(y) \end{cases} \tag{3.8}$$

where the implications come from the linear independence of mass eigenstates $F_{L/R}^n(x^\mu)$. Similarly, for the three other types of $\mathbb{Z}_2$ transformations (2.8)–(2.10), we have the following profile parities:

[16] Those continuity relations lead to $\bar{F}|_0 = \bar{F}|_{0^+}$, i.e., $\bar{F}_\alpha|_0 = \bar{F}_\alpha|_{0^+}$ [c.f. Eq. (B2)], and in turn to $\delta\bar{F}_\alpha|_0 = \delta\bar{F}_\alpha|_{0^+}$ which can be written as $\delta\bar{F}|_0 = \delta\bar{F}|_{0^+}$ via Eq. (B3). Similarly we get $\delta\bar{F}|_{\pi R} = \delta\bar{F}|_{\pi R^-}$.

$$\mathrm{II}\begin{cases} q^n_{L(R)}(-y) = \underset{-}{(+)} q^n_{L(R)}(y) \\ d^n_{L(R)}(-y) = \underset{(-)}{+} d^n_{L(R)}(y) \end{cases}$$

$$\mathrm{III}\begin{cases} q^n_{L(R)}(-y) = \underset{-}{(+)} q^n_{L(R)}(y) \\ d^n_{L(R)}(-y) = \underset{-}{(+)} d^n_{L(R)}(y) \end{cases}$$

$$\mathrm{IV}\begin{cases} q^n_{L(R)}(-y) = \underset{-}{(+)} q^n_{L(R)}(y) \\ d^n_{L(R)}(-y) = \underset{-}{(+)} d^n_{L(R)}(y) \end{cases} \tag{3.9}$$

Therefore, all the $f^n_{L/R}(y)$ profiles are systematically vanishing on the whole $\mathcal{S}^1/\mathbb{Z}_2$ orbifold region, $y \in [-\pi R^+, 0^-] \cup [0, \pi R]$. Such profiles conflict with the two (for L/R) ortho-normalization conditions over the full domain,

$$\forall\, n, m \in \mathbb{N}, \frac{1}{2\pi R}\left(\int_{-\pi R^+}^{0^-} + \int_0^{\pi R}\right) dy f^{n*}_{L/R}(y) f^m_{L/R}(y) = \delta_{nm}, \tag{3.10}$$

originating from the condition of a canonical form for the 4D effective kinetic terms. Hence the solutions for the fields obtained through this first method are not physically consistent.

B. Introducing the EBC

In fact, one necessary ingredient was missing in the naive approach of Sec. III A. In order to identify it, we have to study the conserved fermion probability currents corresponding, via the Noether's theorem, to the global $\mathrm{U}(1)_\mathrm{Q}$ and $\mathrm{U}(1)_\mathrm{D}$ symmetries of the action,

$$S_\mathrm{bulk},$$

involving the Lagrangian (2.5). The two independent global $\mathrm{U}(1)_\mathrm{Q,D}$ transformations of the fields, letting $\mathcal{L}_\mathrm{kin}$ invariant, act respectively as,

$$Q \mapsto \mathrm{e}^{i\alpha} Q, \qquad \bar{Q} \mapsto \mathrm{e}^{-i\alpha} \bar{Q}, \quad \text{and,}$$
$$D \mapsto \mathrm{e}^{i\alpha'} D, \qquad \bar{D} \mapsto \mathrm{e}^{-i\alpha'} \bar{D}, \tag{3.11}$$

where α, α' ($\in \mathbb{R}$) are continuous constants entering for instance the infinitesimal field variations[17]:

$$\underline{\delta} Q = i\alpha Q, \qquad \underline{\delta}\, \bar{Q} = -i\alpha \bar{Q}.$$

Choosing instead to consider a unique symmetry ($\alpha = \alpha'$ for any field F) would correspond to a particular case only, among the general Lagrangian symmetry possibilities. Besides, this particular case would not provide the maximal information, since one symmetry would be associated to only one conserved probability current. We thus well consider, in this subsection, the transformations (3.11) [with both possibilities, $\alpha \neq \alpha'$ or $\alpha = \alpha'$] and the two independent $\mathrm{U}(1)_\mathrm{Q,D}$ symmetries. Based on these two symmetries, and the bulk EOM whose standard structure appears in Eq. (3.1), the Noether's theorem predicts the local conservation relation,

$$\partial_M j^M_F = 0, \tag{3.12}$$

for the two probability currents,

$$j^M_Q = -\alpha \bar{Q} \Gamma^M Q, \qquad j^M_D = -\alpha' \bar{D} \Gamma^M D, \tag{3.13}$$

as derived in details within the Appendix B of Ref. [38]. This relation holds over the whole $\mathcal{S}^1/\mathbb{Z}_2$ orbifold domain, $y \in [-\pi R^+, 0^-] \cup [0, \pi R]$, since the sole bulk terms in the action infinitesimal variation—under $\mathrm{U}(1)_\mathrm{Q,D}$ transformation—must vanish for any integration sub-region included inside the entire integration domain of the action precisely defined for the model. The mathematical consistency of the condition (3.12) imposes necessarily continuous 5-current components over all the model space-time and in particular a continuous j^4_F along $y \in [-\pi R^+, 0^-] \cup [0, \pi R]$.[18] Furthermore, a jump of the form, $j^4_F|_{0^-} \neq j^4_F|_0$, would not determine any field at the fixed point and thus would not lead to vanishing variations in Eq. (3.1) that would modify the BC (3.5) inducing nonphysical solutions. A similar argument applies at the other fixed point, $y = \pi R \equiv -\pi R$. Hence, one has to consider the remaining model possibility, $j^4_F|_{0^-} = j^4_F|_0$ and[19] $j^4_F|_{-\pi R^+} = j^4_F|_{\pi R}$, so that this current component is continuous over all the range, $y \in (-\pi R, \pi R]$. In particular, we can now write,

$$j^4_F|_{0^-} = j^4_F|_0 = j^4_F|_{0^+}. \tag{3.14}$$

This obtained relation must be compared with the following one, coming directly from the $\mathbb{Z}_2$ transformations of type (2.7)–(2.10) and γ^5 properties,

$$\begin{aligned} j^4_F|_{0^-} &= -\alpha^{(\prime)} \bar{F} \Gamma^4 F|_{0^-} = -\alpha^{(\prime)} (\pm\gamma^5 F)^\dagger \gamma^0 [-i\gamma^5] (\pm\gamma^5 F)|_{0^+} \\ &= \alpha^{(\prime)} F^\dagger \gamma^0 \gamma^5 [-i\gamma^5] (\gamma^5 F)|_{0^+} = \alpha^{(\prime)} \bar{F} \Gamma^4 F|_{0^+} = -j^4_F|_{0^+}. \end{aligned} \tag{3.15}$$

The combination of Eqs. (3.14) and (3.15) gives rise to a vanishing current component at the fixed point:

[17] Different clear notations are used here for the infinitesimal field variations under specific transformations, $\underline{\delta} F$, and the above generic field variations in the variation calculus context of the least action principle, δF [see typically Eq. (B3)].

[18] Notice that this condition is in agreement with Eq. (2.3) which guarantees continuous fields along $y \in [-\pi R^+, 0^-] \cup [0, \pi R]$.

[19] A change must occur at both fixed points to cure the problems of the solutions worked out in previous subsection.

$$j^4_F|_{0^-} = j^4_F|_0 = j^4_F|_{0^+} = 0.$$

Similar arguments regarding the second fixed point imply obviously that,

$$j^4_F|_{\pi R^-} = j^4_F|_{\pi R} = j^4_F|_{-\pi R^+} = 0,$$

so that, using the generic chiral decomposition (B5), we get the following current conditions,

$$j^4_F|_{0,\pi R} = i\alpha^{(\prime)}(F^\dagger_L F_R - F^\dagger_R F_L)|_{0,\pi R} = 0, \tag{3.16}$$

leading to the minimal boundary conditions (BC),

$$\begin{cases} F_L|_0 = 0, \\ \quad\text{or} \\ F_R|_0 = 0, \end{cases} \quad \text{and} \quad \begin{cases} F_L|_{\pi R} = 0, \\ \quad\text{or} \\ F_R|_{\pi R} = 0, \end{cases} \quad [\text{EBC}] \tag{3.17}$$

These BC induce systematically the vanishing of all the brane terms in the varied action obtained in Eq. (3.3). Indeed, for example, the fixed value $F_L|_0 = 0$ implies $F^\dagger_L|_0 = 0$ and in turn $\delta F^\dagger_L|_0 = 0$[20] [considering more precisely their two respective components as is clear from Appendix B 1]. Therefore the sole remaining BC are those of Eq. (3.17): there are no more NBC generated from the brane terms of Eq. (3.3) and we name the BC (3.17) as EBC since they are imposed by the $\mathbb{Z}_2$ transformations (3.15) which contribute to define the studied model. From the point of view of the methodology, notice interestingly that it was necessary to consider the fermion probability currents to reveal the existence of the EBC. Now, solving the new EBC (3.17) together with the unchanged bulk EOM (3.4) over the domain, $y \in [0, \pi R]$, was precisely realized in Ref. [38] where the same Eqs. (3.3) and (3.16) [there] were solved over the interval, $y \in [0, L]$. Once more, since the fields are continuous over $y \in [0, \pi R]$ [see Eq. (2.3)] like there over $y \in [0, L]$, we can apply here the results derived in this previous work: the 5D solutions found for Eqs. (3.4)–(3.17) are given by Eqs. (3.6) and (3.7) and the following four possible sets of profiles over $y \in [0, \pi R]$ together with the associated KK mass spectrum equations ($\forall\, n \in \mathbb{N}$),

$$\begin{aligned} &1)\ (--):\ f^n_L(y) = B^n_L \sin(m_n y), (++):\ f^n_R(y) = B^n_L \cos(m_n y);\ \sin(m_n \pi R) = 0, \\ &2)\ (++):\ f^n_L(y) = B^n_R \cos(m_n y), (--):\ f^n_R(y) = -B^n_R \sin(m_n y);\ \sin(m_n \pi R) = 0, \end{aligned} \tag{3.18}$$

and,

$$\begin{aligned} &3)\ (-+):\ f^n_L(y) = B^n_L \sin(m_n y), (+-):\ f^n_R(y) = B^n_L \cos(m_n y);\ \cos(m_n \pi R) = 0, \\ &4)\ (+-):\ f^n_L(y) = B^n_R \cos(m_n y), (-+):\ f^n_R(y) = -B^n_R \sin(m_n y);\ \cos(m_n \pi R) = 0. \end{aligned} \tag{3.19}$$

The opposite signs in front of the $(--)$ and $(-+)$ profiles, with respect to the results in Ref. [38], just come from a different sign convention for the Γ^4 matrix, between here [see Eq. (A3)] and this reference. In Eqs. (3.18) and (3.19), we use the standard BC notations, i.e., $-$ or $+$ for instance at $y = 0$ stands respectively for the Dirichlet or Neumann BC: $f^n_{L/R}(0) = 0$ or $\partial_4 f^n_{L/R}(y)|_0 = 0$. For example, the symbolic notation $(-+)$ denotes Dirichlet (Neumann) BC at $y = 0$ ($y = \pi R$). These notations make explicit the correspondence between the four EBC (3.17) and the four solutions (3.18)–(3.19). The equation $\sin(m_n \pi R) = 0$ possesses the following solutions for the KK mass spectrum,

$$m_n = \pm \frac{n}{R}, \qquad n \in \mathbb{N}. \tag{3.20}$$

Similarly, the equation $\cos(m_n \pi R) = 0$ has the solutions:

$$m_n = \pm \frac{2n+1}{2R}, \qquad n \in \mathbb{N}. \tag{3.21}$$

The part of the general $f^n_{L/R}(y)$ solutions in the complementary domain, $y \in [-\pi R^+, 0^-]$, is now obtained via the four types of $\mathbb{Z}_2$ transformations (3.8)–(3.9). Therefore, the inclusion of the EBC based on the vanishing probability currents allows to obtain consistent fermion profile and mass solutions.

In Table I, we present the explicit solutions over the whole orbifold domain for the SM-like profile $d^n_{L/R}(y)$ ($q^n_{L/R}(y)$) taken from line 1 (2) of Eq. (3.18): see the discussion on SM chirality configuration in Sec. II B 4. The mass spectrum for the 4D KK states is defined by Eq. (3.7) and it is already determined by Eqs. (3.20) and (3.21). Notice on Table I that the same m_n spectrum enters the profile solutions in both regions, $y \in [0, \pi R]$, and, $y \in [-\pi R^+, 0^-]$. In this table, we also give the general values of the $B^n_{L/R}$ complex constants, in Eq. (3.18),

[20]Rigorously speaking, the action should not be minimized with respect to the known fixed fields so that the terms with vanishing field variations should not even appear. In fact, the brane terms of Eq. (3.3) should originally be written as a generic sum over unfixed fields.

obtained from the orthonormalization conditions (3.10).[21] We observe on Table I that the choice of type of $\mathbb{Z}_2$ transformation is just a convention since it can modify the profile signs but it affects neither the mass spectrum nor the fermion chirality configuration—as a certain chiral zero-mode profile vanishing on the region $[0, \pi R]$ is also systematically vanishing over $y \in [-\pi R^+, 0^-]$. In contrast, the chirality configuration and mass spectrum are fixed by the choice of EBC (3.17) which can lead either to the two kinds of chiral solutions in Eq. (3.18) or to the vectorlike solutions (3.19).

In Fig. 2, we draw the first two excitation profiles for each free solution presented in Table I within the simple real case, $\alpha^n_{Q,D} = 0$, and for two different types of $\mathbb{Z}_2$ transformations from Eqs. (3.8) and (3.9). We see clearly on Fig. 2 that for example with the type II of $\mathbb{Z}_2$ transformation, jumps appear for the profiles $q^{0,1}_L(y)$ and $d^{0,1}_R(y)$ at the two fixed points at, $y = 0$, $y = \pi R \equiv -\pi R$, in the scenario without Yukawa couplings. The presence of profile discontinuities here already justifies the treatment exposed in Sec. II A. The precise prescription (2.3) regarding the action integration domain, described in this section, renders the jumps of Fig. 2 consistent mathematically: the difference, e.g., $q^1_L(0^-) \neq q^1_L(0)$, is compatible with a well-defined Lagrangian integrand over the action integration domain, $y \in [-\pi R^+, 0^-] \cup [0, \pi R]$, where the profiles are continuous.

C. Introducing the BBT

As suggested in Sec. II B 4, we can alternatively introduce the dimension 4 operators of Eq. (2.17) to study their effects with respect to the inconsistencies raised in Sec. III A. Hence, to the action $S_{\rm bulk}$ from Eq. (2.4), we add now another part and consider:

$$S_{\rm bulk} + S_B.$$

The variations of S_B with respect to the generic field $\bar{F}$ [using Eq. (B4)],

$$\delta_{\bar{F}} S_B = \int d^4x (\sigma^F_0 \delta F^\dagger_L F_R|_0 + \sigma^F_0 \delta F^\dagger_R F_L|_0 + \sigma^F_{\pi R} \delta F^\dagger_L F_R|_{\pi R} + \sigma^F_{\pi R} \delta F^\dagger_R F_L|_{\pi R}),$$

together with Eq. (3.3) allow to write down the variations of the free fermion action:

$$\delta_{\bar{F}}(S_{\rm bulk} + S_B) = \int d^4x \Bigg\{ \left(\int_{-\pi R^+}^{0^-} + \int_0^{\pi R} \right) dy \delta\bar{F} i\Gamma^M \partial_M F + (\sigma^F_0 1 + 1)\delta F^\dagger_L F_R|_0$$
$$+ (\sigma^F_0 1 - 1)\delta F^\dagger_R F_L|_0 + (\sigma^F_{\pi R} 1 - 1)\delta F^\dagger_L F_R|_{\pi R} + (\sigma^F_{\pi R} 1 + 1)\delta F^\dagger_R F_L|_{\pi R} \Bigg\}. \quad (3.22)$$

The individual vanishing of those volume and surface terms lead to the EOM (3.4) together with the four following NBC, depending on the two $\sigma^F_{0,\pi R}$ choices,

$$\begin{cases} F_L|_0 = 0\,(\sigma^F_0 = -), \\ \qquad \text{or} \\ F_R|_0 = 0\,(\sigma^F_0 = +), \end{cases} \quad \text{and} \quad \begin{cases} F_L|_{\pi R} = 0\,(\sigma^F_{\pi R} = +), \\ \qquad \text{or} \\ F_R|_{\pi R} = 0\,(\sigma^F_{\pi R} = -) \end{cases} \quad [\text{NBC}] \quad (3.23)$$

At this level, the EOM and NBC are effectively the same as the EOM (3.4) and EBC (3.17) of the previous subsection, in the domain $y \in [0, \pi R]$, so that we find again the solutions (3.18)–(3.19) together with the mass spectra (3.20)–(3.21). For instance, the SM-like choice $\sigma^Q_{0(\pi R)} = \underset{(-)}{+}$ of Eq. (2.17) leads via Eq. (3.23) to the solution of line 2 in Eq. (3.18). Then the parts of the general profile solutions in the complementary region, $y \in [-\pi R^+, 0^-]$, are found out via the different types of $\mathbb{Z}_2$ transformations (3.8)–(3.9) in the free case, as in Sec. III B, so that the complete solutions are once more identical and can also be illustrated by the Table I and Fig. 2 both based on the orthonormalization conditions (3.10). In conclusion, introducing the BBT permits to rigorously work out profile and mass solutions. A second conclusion in this approach is that the chirality setup—one of the two chiral solutions (3.18) or of the vectorlike ones (3.19)—and associated mass spectrum are fixed by the choice of NBC (3.23) and thus originally by the choices of $\sigma^F_{0,\pi R}$ BBT signs in Eq. (2.17). In simpler words, the BBT (like the EBC previously) control the chiral nature of the theory as well as each field chirality.

Let us now discuss the probability currents. The addition of the S_B part in Eq. (2.17) to $S_{\rm bulk}$ is not affecting the current equations (3.12) and (3.13) since the new brane

[21]Here, thanks to the profile parities, a change of variable, $y \to -y$, could be applied to recover exclusively the integration domain $[0, \pi R]$.

terms so induced in the infinitesimal action variation—under the $\mathrm{U}(1)_{\mathrm{Q,D}}$ transformations (3.11)—vanish due to their $\mathrm{U}(1)_{\mathrm{Q,D}}$ invariant form. In contrast with the previous subsection and with the interval model in the free case with BBT [38], there exists no demonstration here of Eq. (3.16). Nevertheless, we can check that $j_F^4|_{0,\pi R}$ is well vanishing by using the obtained solutions (3.18) and (3.19): the product $f_L^n(y) f_R^m(y)$ systematically vanishes at $y = 0, \pi R$. Therefore, the BBT play the role of making $j_F^4|_{0,\pi R}$ vanish ($\mathbb{Z}_2$ transformation consequence) like the EBC were guaranteeing it in Sec. III B. Note that we could simultaneously apply the EBC and introduce the BBT but those two processes would be physically redundant to define the model.

IV. BRANE-LOCALIZED SCALAR COUPLINGS IN THE ORBIFOLD: 4D APPROACH

Once the free case is addressed, via the EBC (3.17) in Sec. III B or the NBC (3.23) induced by the BBT in Sec. III C, the free fermion mass spectrum and profiles are known. Then how to take into account the effects of the action part S_X in the mass spectrum, the action (2.15) being induced by the Yukawa interaction between a brane-localized scalar field and bulk fermions? The considered action reads thus as,

$$S_{\text{bulk}} + S_X (+S_B). \tag{4.1}$$

A first method called the perturbation method, described in the present section, is performed at the level of the 4D effective Lagrangian, that is by calculating the mass mixings between the different levels of the KK towers. Considering the SM-like profile solutions $d^n_{L/R}(y)$ ($q^n_{L/R}(y)$) and associated free KK mass spectrum from line 1 (2) of Eq. (3.18), all the initial 4D effective masses for the KK modes of Eq. (3.6) in the interaction basis can be classified into two species: the pure KK masses (3.20) and the mass contributions from the Yukawa interaction given by the overlap between the wave functions and Higgs-brane,

$$\begin{cases} \forall\,(i,j) \in \mathbb{N}^2, & \alpha_{ij} = X \frac{q^i_L(\pi R)}{\sqrt{2\pi R}} \frac{d^j_R(\pi R)}{\sqrt{2\pi R}}, \\ \forall\,(i,j) \in \mathbb{N}^{\star 2}, & \beta_{ij} = X' \frac{d^i_L(\pi R)}{\sqrt{2\pi R}} \frac{q^j_R(\pi R)}{\sqrt{2\pi R}}. \end{cases} \tag{4.2}$$

In particular, $\beta_{ij} = 0$ as imply the respective SM solutions (3.18) so that the coupling constant X' disappears from the mass dependences. Note that for similar reasons [cf., Eq. (B5)], in case of the presence of the BBT (2.17), those do not generate 4D mass terms. All the 4D mass terms enter the 4D effective Lagrangian through the following mass matrix,

$$-\chi_L^\dagger \mathcal{M} \chi_R + \text{H.c.}$$

within the field basis noted,

$$\begin{cases} \chi_L^t(x^\mu) = (Q_L^{0t}, Q_L^{1t}, D_L^{1t}, Q_L^{2t}, D_L^{2t}, \cdots), \\ \chi_R^t(x^\mu) = (D_R^{0t}, Q_R^{1t}, D_R^{1t}, Q_R^{2t}, D_R^{2t}, \cdots). \end{cases} \tag{4.3}$$

The texture of this infinite mass matrix $\mathcal{M}$ involving the diagonal m_n, off-diagonal α_{ij} and mixing the Q, D fields together can be precisely taken from the interval model context [38] (Sec. III.2), with the replacement $L \leftrightarrow \pi R$, since the KK masses and bulk profile solutions are then identical (up to extensions over $[-\pi R^+, 0^-]$ as seen in Sec. III B here) like the Yukawa interactions localized at $y = \pi R$ [for any $\mathbb{Z}_2$ transformation (3.8)–(3.9)]. Now we can apply the results for the mass eigenvalues M_n of the 4D eigenstates $\psi^n_{L/R}(x^\mu)$ obtained through the bi-diagonalization performed in this Ref. [38], based on the calculations of Ref. [53], by renormalizing X to $X/2$ since the two present profiles (even or odd) entering α_{ij} are normalized via Eq. (3.10) over a domain of double size $2L \leftrightarrow 2\pi R$ compared to the interval case. Doing so, the obtained exact mass eigenvalues are determined by the following equation, coming from the characteristic equation,

$$\forall\, n \in \mathbb{N}, \qquad \tan^2\left(\sqrt{|M_n|^2}\pi R\right) = \left(\frac{X}{2}\right)^2, \tag{4.4}$$

in the case of a real X parameter and the positive m_n branch from Eq. (3.20). Notice that the different conventional sign in front of the $(--)$ profiles found in Eq. (3.18) [here $q^n_R(y)$ and $d^n_L(y)$], with respect to the interval study [38], does not affect the final mass spectrum—as is clear from Eq. (4.2). Hence, the physical absolute value of the mass spectrum reads as:

$$|M_n| = \frac{1}{\pi R} \left| \arctan\left(\frac{X}{2}\right) + (-1)^n \tilde{n}(n)\pi \right|, \quad n \in \mathbb{N}, \tag{4.5}$$

with the function $\tilde{n}(n)$ defined according to,

$$\tilde{n}(n) = \begin{cases} \frac{n}{2} & \text{for } n \text{ even}, \\ \frac{n+1}{2} & \text{for } n \text{ odd}. \end{cases} \tag{4.6}$$

V. BRANE-LOCALIZED SCALAR COUPLINGS IN THE ORBIFOLD: 5D APPROACH

A. Applying the NBC

Let us now study the presence of Yukawa couplings at the fixed point, $y = \pi R$, through the action,

$$S_{\rm bulk}+S_X+S_B^0,\quad \text{with},\quad S_B^0=\int d^4x(\sigma_0^Q\bar{Q}Q|_0+\sigma_0^D\bar{D}D|_0), \tag{5.1}$$

within the 5D approach, that is by considering the mixings among KK excitation states at the level of the 5D fields. The BBT introduced here at the fixed point at $y=0$ are the ones of Eq. (2.17) leading to SM-like chirality configurations: $\sigma_0^Q=+$, $\sigma_0^D=-$. Those guarantee a correct treatment of the free brane, like the EBC, as analyzed throughout Sec. III. Using Eqs. (3.22) and (2.15), one gets directly the following action variations with respect to the fields $\bar{Q}$ and $\bar{D}$,

$$\begin{aligned}\delta_{\bar{Q}}(S_{\rm bulk}+S_X+S_B^0)=\int d^4x\bigg\{&\bigg(\int_{-\pi R^+}^{0^-}+\int_0^{\pi R}\bigg)dy\delta\bar{Q}i\Gamma^M\partial_M Q\\&+[\delta Q_L^\dagger(-XD_R-Q_R)+\delta Q_R^\dagger(-X'D_L+Q_L)]|_{\pi R}+2(\delta Q_L^\dagger Q_R)|_0\bigg\},\\ \delta_{\bar{D}}(S_{\rm bulk}+S_X+S_B^0)=\int d^4x\bigg\{&\bigg(\int_{-\pi R^+}^{0^-}+\int_0^{\pi R}\bigg)dy\delta\bar{D}i\Gamma^M\partial_M D\\&+[\delta D_L^\dagger(-X'^*Q_R-D_R)+\delta D_R^\dagger(-X^*Q_L+D_L)]|_{\pi R}-2(\delta D_R^\dagger D_L)|_0\bigg\}.\end{aligned} \tag{5.2}$$

The separate vanishings of these volume and surface terms, induced by the least action principle, give rise respectively to the EOM (3.4) and the following NBC,

$$\begin{cases}(Q_R+XD_R)|_{\pi R}=0,\quad (D_L-X^*Q_L)|_{\pi R}=0,\\ (Q_L-X'D_L)|_{\pi R}=0,\quad (D_R+X'^*Q_R)|_{\pi R}=0,\\ Q_R|_0=0, D_L|_0=0,\end{cases} \tag{5.3}$$

As usual, the 5D field solutions of the EOM (3.4) and NBC (5.3) have the form of the following mixed KK decomposition [instead of Eq. (3.6)] [5,44],

$$\begin{bmatrix} Q_L(x^\mu,y)=\frac{1}{\sqrt{2\pi R}}\sum_{n=0}^{+\infty}q_L^n(y)\psi_L^n(x^\mu),\\ Q_R(x^\mu,y)=\frac{1}{\sqrt{2\pi R}}\sum_{n=0}^{+\infty}q_R^n(y)\psi_R^n(x^\mu),\\ D_L(x^\mu,y)=\frac{1}{\sqrt{2\pi R}}\sum_{n=0}^{+\infty}d_L^n(y)\psi_L^n(x^\mu),\\ D_R(x^\mu,y)=\frac{1}{\sqrt{2\pi R}}\sum_{n=0}^{+\infty}d_R^n(y)\psi_R^n(x^\mu),\end{bmatrix} \tag{5.4}$$

with the 4D fields $\psi_{L/R}^n(x^\mu)$, already mentioned in Sec. IV, satisfying the Dirac-Weyl equations,

$$\begin{cases}i\bar{\sigma}^\mu\partial_\mu\psi_L^n(x^\mu)-M_n\psi_R^n(x^\mu)=0,\\ i\sigma^\mu\partial_\mu\psi_R^n(x^\mu)-M_n\psi_L^n(x^\mu)=0,\end{cases} \tag{5.5}$$

the M_n being the fermion mass eigenvalues including the contributions from the Yukawa terms and these 4D fields the mass eigenstates including the effects of mixings among the Q, D fields as well as (infinite) KK levels. The explicit profile solutions appearing in Eq. (5.4) over the domain, $y\in[0,\pi R]$, were found out for the interval model studied in Ref. [38] where the exactly identical EOM and same NBC, up to a sign and a factor 2 in front of each $X^{(\prime)}$ parameter, [respectively Eq. (3.3) and (5.5) there] have been solved over $y\in[0,L]$. Because the fields are continuous over $y\in[0,\pi R]$ [cf., Eq. (2.3)] like there over $y\in[0,L]$, one can apply here the conclusions obtained in this reference. The opposite sign in front of the $X^{(\prime)}$ parameters originates from a different Dirac matrix sign convention [see the Γ^4 sign in Eq. (A3)] and has thus no physical consequences. The relative factors 2, at the same places in the NBC (5.3), come from the existence of surface terms both at $y=0$, 0^- and $y=\pi R$, $-\pi R^+$ as is clearly described in Eq. (3.1)–(3.3). These factors turn out not to modify the relations between the different profile solutions and to only induce a factor-4 change in the final mass spectrum equation, both obtained in Ref. [38]. Besides, the two (for L/R) following orthonormalization conditions over the full $\mathcal{S}^1$ domain [replacing Eq. (3.10)],

$$\begin{aligned}\forall\, n,m\in\mathbb{N},\frac{1}{2\pi R}\bigg(\int_{-\pi R^+}^{0^-}+\int_0^{\pi R}\bigg)dy[q_{L/R}^{n*}(y)q_{L/R}^m(y)\\ +d_{L/R}^{n*}(y)d_{L/R}^m(y)]=\delta_{nm},\end{aligned} \tag{5.6}$$

as induced by the decomposition (5.4), can be recast into the integration relations of Ref. [38] over the region $[0,\pi R]$ but with a global factor 2, thanks to the change of variable $y'=-y$, the fixed odd/even parities of the profiles and Eq. (2.3), so that the demonstration about profile solutions on the interval in Ref. [38] remains unchanged here, from this point of view as well. Indeed, injecting the mixed KK decomposition (5.4) into the first type of $\mathbb{Z}_2$ transformation (2.7), we get the $\mathbb{Z}_2$ transformations directly on the profiles:

$$\text{Type I}\begin{cases}\sum_{n=0}^{+\infty}[q^n_{L(R)}(-y)\underset{-}{(+)}q^n_{L(R)}(y)]\psi^n_{L(R)}(x^\mu)=0\Rightarrow q^n_{L(R)}(-y)=\underset{(-)}{+}q^n_{L(R)}(y)\\ \sum_{n=0}^{+\infty}[d^n_{L(R)}(-y)\underset{(-)}{+}d^n_{L(R)}(y)]\psi^n_{L(R)}(x^\mu)=0\Rightarrow d^n_{L(R)}(-y)=d^n_{L(R)}(y)\end{cases}\tag{5.7}$$

In the same way, for the three other types of $\mathbb{Z}_2$ transformations (2.8)–(2.10), one obtains the same profile parities as in Eq. (3.9). As a conclusion, the same result as in Ref. [38] holds here for the orbifold: the 4D effective Yukawa coupling constant for the lightest modes ($\psi^0_{L,R}$), induced by the found profiles, tends to zero within the decoupling limit which is not compatible with the SM configuration expected. The problematic characteristics of the solutions obtained in this naive approach are confirmed by the final mass spectrum equation, $\tan^2(M_n\pi R)=|X|^2$ (independent from the profile normalizations), which conflicts analytically with the one obtained through the 4D method in Eq. (4.4) for a real X parameter. This failure motivates the alternative 5D methods of the next two subsections.

B. Introducing the EBC

Following the same idea as for the free case in Sec. III B, we try now to find consistent fermion mass solutions via considerations on their currents. The currents permit *a priori* to fully define the geometrical field configuration like here for the $\mathcal{S}^1/\mathbb{Z}_2$ orbifold scenario. The complete relevant action including the brane-localized Yukawa terms (2.15),

$$S_{\rm bulk}+S_X+S_B^0,\tag{5.8}$$

like in Eq. (5.1), is invariant under the unique $\mathrm{U}(1)_\mathrm{F}$ symmetry defined via Eq. (3.11) only for,

$$\alpha=\alpha',\tag{5.9}$$

since the fermions Q and D are mixed on the brane at $y=\pi R$. Based on this symmetry involving both Q and D as well as on the bulk EOM [whose standard structure appears in the action variation (3.1)], the Noether's theorem predicts (cf., Appendix B of Ref. [38]) the new local probability conservation relation,

$$\partial_M j^M=0,\quad \text{with},\quad j^M=\sum_{F=Q,D}j^M_F,\tag{5.10}$$

involving the individual currents given by Eqs. (3.13)–(5.9) over the full orbifold domain, $y\in[-\pi R^+,0^-]\cup[0,\pi R]$. Notice that the new S_X brane terms entering the infinitesimal action variation—under the $\mathrm{U}(1)_\mathrm{F}$ transformations—vanish because of their invariant form and have thus no direct effect on the conservation relation (5.10). The mathematical consistency of the relation (5.10) implies necessarily the continuity of 5-current components over the whole space-time and in particular a continuous j^4 along $y\in[-\pi R^+,0^-]\cup[0,\pi R]$. Besides, a discontinuity of the form, $j^4|_{-\pi R^+}\neq j^4|_{-\pi R}\equiv j^4|_{\pi R}$, would not fix any field at this fixed point and in turn would not induce vanishing variations in Eq. (5.2) possibly modifying the BC (5.3) which induce the drawbacks already pointed out in Sec. V A. As a consequence, we must consider the remaining model possibility:

$$j^4|_{-\pi R^+}=j^4|_{-\pi R}\equiv j^4|_{\pi R}=j^4|_{\pi R^-},\tag{5.11}$$

where Eq. (2.3) is also invoked. On the other side, the current j^4 is odd under any type of $\mathbb{Z}_2$ transformation (2.7)–(2.10) as can be shown in a similar way as in Eq. (3.15):

$$j^4|_{-\pi R^+}=-j^4|_{\pi R^-}.\tag{5.12}$$

Combining Eq. (5.11) with Eq. (5.12) leads to,

$$j^4|_{\pi R^-}=j^4|_{\pi R}=j^4|_{-\pi R^+}=0,$$

so that, using Eqs. (3.16) and (5.9), we get the relation (inducing EBC),

$$j^4|_{\pi R}=i\alpha(Q_L^\dagger Q_R-Q_R^\dagger Q_L+D_L^\dagger D_R-D_R^\dagger D_L)|_{\pi R}=0,\tag{5.13}$$

and its variation (for a nontrivial transformation with $\alpha\neq 0$),

$$\begin{aligned}&(\delta Q_L^\dagger Q_R+Q_L^\dagger\delta Q_R-\delta Q_R^\dagger Q_L-Q_R^\dagger\delta Q_L\\&\quad+\delta D_L^\dagger D_R+D_L^\dagger\delta D_R-\delta D_R^\dagger D_L-D_R^\dagger\delta D_L)|_{\pi R}=0.\end{aligned}\tag{5.14}$$

At this level, we can consider the search for field solutions of vanishing Eqs. (5.2) and (5.13)–(5.14) first on the domain, $y\in[0,\pi R]$, which is equivalent to the search performed for the interval model in Ref. [38] with the replacement, $L\leftrightarrow\pi R$. Given that the orthonormalization condition (5.6) written on the domain $[0,\pi R]$ is the same within the orbifold and interval frameworks, up to an overall factor 2, we can apply the conclusion of Ref. [38] and claim that there exists no SM-like consistent solution for the fields (over $y\in[0,\pi R]$) for similar reasons as in Sec. V A. As a conclusion, the introduction of EBC does not constitute the correct approach towards the treatment of point-like Yukawa interactions at a fixed point of the $\mathcal{S}^1/\mathbb{Z}_2$ orbifold. Regarding the bulk fermion probability currents, both the cases of a j^4 jump and a j^4 continuity at the Yukawa coupling location, $y = \pi R$, lead to inconsistent field solutions so that, at this stage of the study, there exists no theoretical proof of the j^4 continuity—and via Eq. (5.12) of its vanishing—at this fixed point, in contrast with the interval model (case of presence of boundary-localized Yukawa interactions) [38].

C. Introducing the BBT

In order to get meaningful field solutions in the presence of brane-localized Yukawa couplings at the fixed point, $y = \pi R$, let us finally try the introduction of the SM-like BBT (2.17) as in the free case of Sec. III C or as in the interval model [38]. We thus consider here the same action as in Eqs. (5.1)–(5.8) but adding now the BBT at $y = \pi R$:

$$S_{\text{bulk}} + S_X + S_B.$$

Using Eqs. (3.22) and (5.2), we find the following action variations with respect to $\bar{Q}$ and $\bar{D}$:

$$\begin{aligned}
\delta_{\bar{Q}}(S_{\text{bulk}} + S_X + S_B) = \int d^4x \bigg\{ \bigg(\int_{-\pi R^+}^{0^-} + \int_0^{\pi R} \bigg) dy \delta\bar{Q} i\Gamma^M \partial_M Q \\
+ \bigg[-2\delta Q_L^\dagger \bigg(Q_R + \frac{X}{2} D_R \bigg) - X' \delta Q_R^\dagger D_L \bigg] \bigg|_{\pi R} + 2(\delta Q_L^\dagger Q_R)|_0 \bigg\}, \\
\delta_{\bar{D}}(S_{\text{bulk}} + S_X + S_B) = \int d^4x \bigg\{ \bigg(\int_{-\pi R^+}^{0^-} + \int_0^{\pi R} \bigg) dy \delta\bar{D} i\Gamma^M \partial_M D \\
+ \bigg[-X'^* \delta D_L^\dagger Q_R + 2\delta D_R^\dagger \bigg(D_L - \frac{X^*}{2} Q_L \bigg) \bigg] \bigg|_{\pi R} - 2(\delta D_R^\dagger D_L)|_0 \bigg\}.
\end{aligned}$$

The individual vanishing of those volume and surface terms, due to the action minimization, leads to the EOM (3.4) and the following NBC,

$$\begin{cases} \{Q_R + (X/2)D_R\}|_{\pi R} = 0, \quad \{D_L - (X^*/2)Q_L\}|_{\pi R} = 0, \\ X' D_L|_{\pi R} = 0, \quad X'^* Q_R|_{\pi R} = 0, \quad Q_R|_0 = D_L|_0 = 0, \end{cases} \tag{5.15}$$

which differ from the NBC (5.3) obtained without the BBT. As before, given the continuity region defined by Eq. (2.3), we can start by considering the search for profile solutions of 5D EOM (3.4) and 5D NBC (5.15) on the domain, $y \in [0, \pi R]$, being equivalent to the search performed for the interval scenario (with BBT) [38] after the replacement, $L \leftrightarrow \pi R$. The 4D field solutions in the decomposition (5.4) obey the known Eq. (5.5). First, the opposite sign in factor of each $X^{(\prime)}$ parameter in the NBC (5.15), with respect to Ref. [38] [see Eq. (5.23) there], comes from the mentioned different Dirac matrix sign convention [cf., Γ^4 in Eq. (A3)] and hence has no physical impact, neither on the fermion masses nor on the 4D effective Yukawa couplings [see Eq. (5.21)]. Second, the factor $1/2$ difference at the same places in NBC (5.15), compared to the interval NBC [38], comes from the existence of double numbers of surface terms (at $y = 0$, 0^- and $y = \pi R$, $-\pi R^+$)—like in Sec. V A—and leads to the factor $1/2$ in the final mass spectrum relations (5.18)–(5.19) through a renormalization of the X parameter as $X/2$. Thirdly, the necessary orthonormalization condition (5.6) can be rewritten on the domain $[0, \pi R]$ only, as [the subscript C stands for L or R],

$$\delta_{nm} = \frac{1}{\pi R} \int_0^{\pi R} dy [q_C^{n*}(y) q_C^m(y) + d_C^{n*}(y) d_C^m(y)], \tag{5.16}$$

thanks to the change of variable, $y' = -y$, the fixed profile parities (5.7)–(3.9) and the continuity relations (2.3):

$$\begin{aligned}
\int_{-\pi R^+}^{0-} dy [q_C^{n*}(y) q_C^m(y) + d_C^{n*}(y) d_C^m(y)] = \int_{0^+}^{\pi R^-} dy' [q_C^{n*}(-y') q_C^m(-y') + d_C^{n*}(-y') d_C^m(-y')] \\
= \int_{0^+}^{\pi R^-} dy' [q_C^{n*}(y') q_C^m(y') + d_C^{m*}(y') d_C^m(y')] = \int_0^{\pi R} dy [q_C^{n*}(y) q_C^m(y) + d_C^{n*}(y) d_C^m(y)],
\end{aligned}$$

recovering thus exactly and conveniently the interval condition, if $L = \pi R$. Nevertheless, including the factor $1/\sqrt{2\pi R}$, the dimensional wave functions [mass dimension $1/2$] are identical within the orbifold and interval frameworks only up to an additional normalization factor $1/\sqrt{2}$ here, due to the double compact space size: see the respectively used decomposition normalizations (5.4) above and (4.1) in Ref. [38]. Therefore, we can finally apply the results of Ref. [38] here for the SM-like consistent solutions of the fields over $y \in [0, \pi R]$: we find, for the dimensionless profiles ($\forall\, n \in \mathbb{N}$),

$$\begin{cases} (+\times):\ q_L^n(y) = A_q^n \cos(M_n y), & (-\times):\ q_R^n(y) = -A_q^n \sin(M_n y), \\ (-\times):\ d_L^n(y) = A_d^n \sin(M_n y), & (+\times):\ d_R^n(y) = A_d^n \cos(M_n y), \end{cases} \tag{5.17}$$

for the two classes of real mass spectrum solutions ($X = |X|e^{i\alpha_Y}$ with $\alpha_Y,\ \alpha_0^n \in \mathbb{R}$),

$$\tan(M_n \pi R) = \left|\frac{X}{2}\right|, \qquad A_q^n = e^{i(\alpha_0^n + \alpha_Y)}, \qquad A_d^n = e^{i\alpha_0^n}, \tag{5.18}$$

$$\tan(M_n \pi R) = -\left|\frac{X}{2}\right|, \qquad A_q^n = e^{i(\alpha_0^n + \alpha_Y \pm \pi)}, \qquad A_d^n = e^{i\alpha_0^n}, \tag{5.19}$$

and for the absolute values of the fermion masses [based on Eq. (4.6)],

$$|M_n| = \frac{1}{\pi R}\left|\arctan\left|\frac{X}{2}\right| + (-1)^n \tilde{n}(n)\pi\right|. \tag{5.20}$$

We call $(\times)$ the new Yukawa coupling (in X) dependent BC, given by Eqs. (5.17)–(5.19), (5.20) at the brane located at $y = \pi R$, in order to distinguish them from the Dirichlet BC usually noted $(-)$ and the Neumann BC $(+)$. Note that, similarly to the free solutions (3.18), the opposite signs in front of the $(-\times)$ profiles (5.17), with respect to the results of Ref. [38], simply come from a different sign convention for the Γ^4 matrix. At this stage, the part of the profile solutions on the complementary region, $y \in [-\pi R^+, 0^-]$, is deduced through the four types of $\mathbb{Z}_2$ transformations (5.7)–(3.9). Hence, the M_n spectrum entering the profile solutions in both regions, $[0, \pi R]$ and $[-\pi R^+, 0^-]$, is the same. As a first conclusion, the introduction of the BBT allows to obtain realistic fermion wave functions and consistent mass eigenvalues. The absolute mass spectrum obtained within the 5D approach in Eq. (5.20) is analytically matching the one derived via the 4D method in Eq. (4.5) for a real Yukawa coupling constant: this feature represents a nontrivial confirmation of the present exact results. In particular, the absence of X' parameter in the fermion 4D mass matrix $\mathcal{M}$, described below Eq. (4.2), is interestingly recovered through the mass independence from X' as induced as well by the condition

$$X' = 0,$$

issued from the 5D NBC (5.15). Regarding the probability current, the component $j^4|_{\pi R}$ at the Yukawa brane is still given by Eq. (5.13) since the BBT do not affect it, as explained at the end of Sec. III C. The relations found in the first line of the NBC (5.15), injected once into each term of this current component expression, give rise to,

$$j^4|_{\pi R} = 0.$$

The BBT are thus found to induce NBC leading to a vanishing current component along the extra dimension at

TABLE II. SM-like coupled fermion profiles on the two orbifold continuity domains $[-\pi R^+, 0^-]$ and $[0, \pi R]$, corresponding to the solutions (5.17), (5.18)–(5.19), together with the associated absolute mass spectrum (5.20) for completeness. The profiles are given for the four types of $\mathbb{Z}_2$ transformations (5.7)–(3.9).

Continuity domains	$\mathbb{Z}_2$	Fields: $Q_{L/R}$ $q_L^n(y)/(\pm e^{i(\alpha_0^n+\alpha_Y)})$	Fields: $Q_{L/R}$ $q_R^n(y)/(\pm e^{i(\alpha_0^n+\alpha_Y)})$	Fields: $D_{L/R}$ $d_L^n(y)/e^{i\alpha_0^n}$	Fields: $D_{L/R}$ $d_R^n(y)/e^{i\alpha_0^n}$
$[0, \pi R]$	Any	$\cos(M_n y)$	$-\sin(M_n y)$	$\sin(M_n y)$	$\cos(M_n y)$
$[-\pi R^+, 0^-]$	I	$\cos(M_n y)$	$-\sin(M_n y)$	$\sin(M_n y)$	$\cos(M_n y)$
	II	$-\cos(M_n y)$	$\sin(M_n y)$	$-\sin(M_n y)$	$-\cos(M_n y)$
	III	$\cos(M_n y)$	$-\sin(M_n y)$	$-\sin(M_n y)$	$-\cos(M_n y)$
	IV	$-\cos(M_n y)$	$\sin(M_n y)$	$\sin(M_n y)$	$\cos(M_n y)$
KK Masses		$\lvert M_n\rvert = \lvert\arctan\lvert X/2\rvert + (-1)^n \tilde{n}(n)\pi\rvert/\pi R,\ n \in \mathbb{N}$			

the fixed points of the orbifold, with (present section) or without (cf., Sec. III C) a brane-localized Yukawa coupling, and in turn to a continuous current component along the extra dimension at those points given the odd parities, demonstrated in Eq. (5.12) or (3.15) respectively.

In Table II are exhibited the explicit profile functions over the entire orbifold domain for the SM-like solutions (5.17), (5.18)–(5.19), (5.20). We can see on this table that the choice of type of $\mathbb{Z}_2$ transformation is purely a convention because it can modify the profile signs but without effects on the mass spectrum.

In Fig. 3, we illustrate a set of excitation profiles, obeying the $\mathbb{Z}_2$ transformations of types I and II in Eqs. (5.7)–(3.9), for the found Yukawa-coupled solutions (5.18), which are explicitly presented in Table II, within the simplified real case, $\alpha_Y = \alpha_0^n = 0$. We observe on this figure that all the wave function values at the Yukawa-brane (at the fixed point, $y = \pi R$) are modified due to the presence of this coupling. For example, under the type I of $\mathbb{Z}_2$ transformation, the profile values $d_L^n(\pi R) = d_L^n(\pi R^-)$ are shifted from zero as well as from $d_L^n(-\pi R^+)$, in contrast with the free case shown in Fig. 2. This shift creates profile jumps whose amplitude is depending on the Yukawa coupling constant through the X parameter [BC $(\times)$ from Eq. (5.17), (5.18)–(5.19), (5.20)]. Under the type II of $\mathbb{Z}_2$ transformation, the same figure shows clearly that the profile jump $d_L^n(\pi R) = d_L^n(\pi R^-) \neq d_L^n(-\pi R^+)$ disappears but then other kinds of jump arise like: $q_L^n(\pi R) = q_L^n(\pi R^-) \neq q_L^n(-\pi R^+)$ and $q_L^n(0^-) \neq q_L^n(0) = q_L^n(0^+)$. The presence of new possible profile discontinuities justifies once more mathematically the prescriptions about the field continuities and action integration domains introduced in Sec. II A.

Finally, let us calculate, still without any kind of Higgs field regularization, the physical 4D effective Yukawa coupling constants between the mass eigenstates $\psi_L^n(x^\mu)$ and $\psi_R^m(x^\mu)$ as generated by the insertion of decompositions (5.4) into Eq. (2.16), based on the obtained profile expressions (5.17), (5.18)–(5.20):

$$\begin{aligned} y_{nm} &\hat{=} -\frac{Y_5}{2\sqrt{2}\pi R} q_L^{n*}(\pi R) d_R^m(\pi R) \\ &= \mp \frac{|Y_5|}{2\sqrt{2}\pi R} e^{i(\alpha_0^m - \alpha_0^n)} \cos(M_n \pi R)\cos(M_m \pi R) \\ &= \mp (-1)^{\tilde{n}(n)+\tilde{n}(m)} e^{i(\alpha_0^m - \alpha_0^n)} \frac{|Y_5|}{2\sqrt{2}\pi R(1+|X/2|^2)}, \end{aligned} \tag{5.21}$$

where we have used a trigonometric identity[22] to get the last equality. In the decoupling limit of extremely heavy KK modes, $R \to 0$, we can then write the modulus of the lightest mode coupling constant, using Eq. (2.14), as,

$$\begin{aligned} |y_{00}| &\underset{R\to 0}{\to} \frac{|Y_5|}{2\sqrt{2}\pi R} = \frac{|y_4|}{\sqrt{2}}, \quad \text{since ,} \\ X &= \frac{v}{\sqrt{2}} Y_5 = \frac{v}{\sqrt{2}} 2\pi R y_4, \end{aligned} \tag{5.22}$$

and the absolute mass eigenvalue of the lightest eigenstates as [from Eq. (5.20)],

$$|M_0| \underset{R\to 0}{\to} \frac{|X|}{2\pi R} = \frac{v|Y_5|}{2\sqrt{2}\pi R} \underset{R\to 0}{\to} v|y_{00}|, \tag{5.23}$$

so that the SM fermion setup—for the assumed single family—is recovered as expected from the decoupling condition. Besides, we can conclude that the choice of type of $\mathbb{Z}_2$ transformation among Eqs. (5.7)–(3.9) affects neither the profile values taken at the point $y = \pi R$—see Table II—nor their global orthonormalization condition (5.6)—as described right below Eq. (5.16)—so that the 4D effective Yukawa coupling constants (5.21) are insensitive as well to this $\mathbb{Z}_2$ representation choice.

VI. THE INCLUSIVE $\mathbb{Z}_2$ PARITY

Let us study the alternative scenario whose definition is based on the $\mathbb{Z}_2$ transformation of 5D fields extended to include the two fixed points at $y = 0$ and $y = \pi R$:

$$\Phi(x^\mu, -y) = \mathcal{T}\Phi(x^\mu, y), \quad \forall\, y \in (-\pi R, \pi R], \tag{6.1}$$

in contrast with Eq. (2.1). This generic transformation still lets the Lagrangian density invariant, exactly like in Eq. (2.2). At the two fixed points, this Lagrangian invariance is once more automatically satisfied without the need for any specific $\mathcal{T}$ transformation. Accordingly to the simple Eq. (6.1), the operator $\mathcal{T}$ for the fixed points is the same as the non-trivial one which must let the Lagrangian invariant in the bulk. Let us consider in particular the realistic $\mathbb{Z}_2$ transformation leading to the SM chirality setup: it is the bulk transformation in Eq. (2.7), defined now over the same range as in Eq. (6.1), which keeps well $\mathcal{L}_{\rm kin}$ invariant in the bulk according to Eq. (2.2):

$$\begin{cases} Q(x^\mu, -y) = -\gamma^5 Q(x^\mu, y) \\ D(x^\mu, -y) = \gamma^5 D(x^\mu, y) \end{cases}, \quad \forall\, y \in (-\pi R, \pi R]. \tag{6.2}$$

Focusing on the fixed points at $y = 0$ and $y = \pi R \equiv -\pi R$, we obtain the four nontrivial relations

[22] For $n \in \mathbb{Z}$, one has, $\cos(\theta + n\pi) = (-1)^n \cos(\theta)$, and for $T \in \mathbb{R}$, $\cos[\arctan(T)] = \frac{1}{\sqrt{1+T^2}}$.

$$\begin{cases} Q(x^\mu,0) = -\gamma^5 Q(x^\mu,0) \Rightarrow Q_L|_0 = Q_L|_0, \quad \text{and,} \quad Q_R|_0 = -Q_R|_0 = 0 \\ D(x^\mu,0) = \gamma^5 D(x^\mu,0) \Rightarrow D_L|_0 = -D_L|_0 = 0, \quad \text{and,} \quad D_R|_0 = D_R|_0 \end{cases} \tag{6.3}$$

$$\begin{cases} Q(x^\mu,\pi R) = -\gamma^5 Q(x^\mu,\pi R) \Rightarrow Q_R|_{\pi R} = 0 \\ D(x^\mu,\pi R) = \gamma^5 D(x^\mu,\pi R) \Rightarrow D_L|_{\pi R} = 0 \end{cases} \quad [\text{EBC}']$$

representing new EBC that we denote EBC' to distinguish them from those in Eq. (3.17).

In the free case, Sec. III A has shown that EBC(') or BBT must be considered. Starting with the EBC('), in analogy with Sec. III B, the fixed $\mathbb{Z}_2$ transformations (6.2) in the bulk lead to the EBC (3.17) while the $\mathbb{Z}_2$ transformations (6.3) at the fixed points lead to the EBC'. Those EBC' select one general BC set among these four EBC sets for the 5D field Q, and same statement for D: the sets corresponding to the chiral solution of line 1 (2) in Eq. (3.18) for the field D (Q), namely the SM-like chirality configuration. Finally, the complete profile solutions over the whole orbifold domain are found out as before via the bulk $\mathbb{Z}_2$ transformations (6.2).

Alternatively, the selected consistent BBT (2.17) can be included like in Sec. III C to obtain the same SM-like solutions. The corresponding EBC' (6.3), part of the EBC (3.17) and required by the model, are checked to be satisfied afterwards, as consequences.

Once the free profiles are worked out as described right above—either through the EBC(') or the BBT—we can apply the 4D method of Sec. IV, based on infinite matrix diagonalization, in order to derive the mass spectrum in the presence of brane-localized Yukawa couplings. Even the 4D effective Yukawa coupling constants can be calculated in this way: the above EBC' selection of a specific chirality setup and mass spectrum for the free fields would affect as well these effective coupling constants, for instance via the KK mass mixings.

In contrast, the analysis of pointlike Yukawa interactions cannot be achieved via the 5D approach within the present inclusive $\mathbb{Z}_2$ symmetry model.

First, the EBC(') motivated by Sec. V A must be split into the EBC coming directly from the vanishing probability currents—or say indirectly from the fixed $\mathbb{Z}_2$ transformations (6.2) in the bulk—discussed in Sec. V B and the EBC' (6.3). These EBC' combined with the surface terms at $y = \pi R$ in Eq. (5.2), including the Yukawa terms, give rise to the BC of type (5.3) involving only single terms proportional to the Yukawa coupling constant and equal to zero. Hence, the resulting mass spectrum loses its dependence on the Yukawa coupling constant which conflicts with the decoupling limit argument [see Eq. (5.23)].

Second, the BBT (2.17) could be added like in Sec. V C to try obtaining SM-like solutions. However the EBC' (6.3), expected to be recovered afterwards, are not compatible with the resulting BC (5.17) together with the spectrum equations (5.18) and (5.19).

VII. RESULT ANALYSIS

A. The higher-dimensional method

The present study confirms the general methodology depicted in Fig. 4 and presented in Ref. [38]. Within the present model, the probability current condition on this schematic description is the vanishing of fermion currents at the two fixed points (issued from $\mathbb{Z}_2$ symmetry criteria and inducing the EBC (3.17) in the free case). For the interval model, the vanishing current condition is a direct implication of the existence of boundaries for the matter fields. This current vanishing holds both in the presence and absence of brane-localized Yukawa couplings.

In the framework of the orbifold version described in Sec. VI, the additional field condition (6.3), coming from the $\mathbb{Z}_2$ symmetry at the fixed points, accompanies the definition of the $\mathbb{Z}_2$ symmetry of the bulk action and leads to the new EBC'.

B. Discussion of the action content

In addition to the information contained in the action (2.18), the present orbifold model is defined in a complementary way by other elements like: (i) the $\mathcal{S}^1$ junction point at $y = \pi R \equiv -\pi R$, (ii) the choices of $\mathbb{Z}_2$ transformations for the fields in the bulk [see Eqs. (2.7)–(2.10)] and possibly at the fixed points [cf., Eq. (6.3)], (iii) the EBC (3.17) imposed by the model definition when those are used instead of the BBT. Regarding the point (iii), Table III summarizes the obtained cases where the EBC and

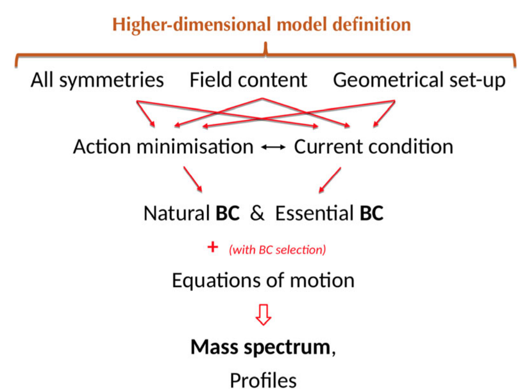

FIG. 4. Schematic inverse pyramidal picture describing the generic process for determining the mixed KK mass spectrum and bulk field wave functions. Acronym notations are the same as in the main text.

TABLE III. Types of boundary conditions for the bulk fermions at an orbifold fixed point where is located their interactions with the Higgs boson, in different brane treatments: presence of BBT, vanishing of probability current or nothing specific. The 4D line holds as well for the 5D approach of the free brane. As usually, the Dirichlet BC are noted $(-)$, the Neumann BC $(+)$ and we denote $(\times)$ the new BC depending on the Yukawa coupling constant [corresponding to Eq. (5.17) taken at $y = \pi R$]. The (N,E)BC acronym definitions are the same as in the text.

	No boundary characteristic	Vanishing current condition [EBC]	Bilinear brane terms [NBC]
4D Approach	*(Impossible)*	BC $(\pm)$	BC $(\pm)$
5D Approach	*(Impossible)*	*(Impossible)*	BC $(\times)$

the BBT can be used. This table is identical to the one obtained in the interval model study [38].

C. About the orbifold/interval duality

The present $\mathcal{S}^1/\mathbb{Z}_2$ orbifold model and the $[0, L]$ interval scenario studied in Ref. [38] are physically different: their geometrical setups and Lagrangian symmetries are not identical. Nevertheless, the respective theoretical predictions for the observables like the (brane-coupled) fermion mass spectra and 4D effective Yukawa coupling constants are identical up to factors 2, which may be called a duality. Indeed, for a comparable dimension size $L = \pi R$, although the mass absolute values (5.20) involve a new factor $1/2$ in front of X, with respect to the interval analytical result, the measurable range of values for $|M_n|$ is of the same order and the precise limits of this range rely on the approximate perturbative limits of the 4D effective Yukawa coupling constants proportional to y_4 [see Secs. II B 3 and Eqs. (5.21)–(5.23)]. Besides, the dependence of the analytical mass formula on the Lagrangian parameters is identical in the two models, up to this factor $1/2$ entering the coupling constant definition, as can be seen from Eq. (5.20) and Sec. II B 3—including the free limiting case $X \to 0$. Similar comments hold for the 4D effective Yukawa coupling constants (5.21) which have additional factors $1/2$ in front of X and as an overall factor (latter one induced by normalization considerations), with respect to the interval case.

The orbifold version of Sec. VI contains additional information at the fixed point branes. It predicts thus a specific chirality configuration and mass spectrum [among chiral or vector-like solutions respectively of type (3.18)–(3.19)] so that it is not dual to the interval model.

Coming back to the case of duality, there exist similarities between the orbifold and interval models, as it appeared throughout this work when solving the EOM and BC to find out the fields. Let us now comment on the similarities at the Lagrangian level. First, the BBT (2.17) have the same form as in the interval framework [38] and the different factor 2 is related to the double size of the compactified space for the identification, $L = \pi R$. The opposite front sign in the BBT (for a similar profile solution setup) is just due to a different Dirac matrix sign convention [see Γ^4 sign in Eq. (A3)].

In the global action (2.18), S_{bulk} remains to be discussed, the other parts being identical in the orbifold and interval models. Thanks to the orbifold property (2.2), the change of variable, $y' = -y$, allows the following rewriting of Eq. (2.4),

$$\begin{aligned} S_{\text{bulk}} &= \int d^4x \left(\int_{-\pi R^+}^{0^-} dy \mathcal{L}_{\text{kin}}(y) + \int_0^{\pi R} dy \mathcal{L}_{\text{kin}}(y) \right) \\ &= \int d^4x \left(\int_{0^+}^{\pi R^-} dy' \mathcal{L}_{\text{kin}}(y') + \int_0^{\pi R} dy \mathcal{L}_{\text{kin}}(y) \right) \\ &= 2 \int d^4x \left(\int_0^{\pi R} dy \mathcal{L}_{\text{kin}}(y) \right), \end{aligned} \tag{7.1}$$

where the last step is based on Eq. (2.3). Therefore, using Eq. (2.18) and the relevant identification, $L = \pi R$, we can express the orbifold action in terms of the interval action pieces [38] (indicated by the L exponent):

$$\begin{aligned} S_{5D} &= 2S_{\text{bulk}}^L + S_H^{(L)} + S_X^{(L)} + S_{\text{int}}^{(L)} + 2S_B^L \\ &= 2[S_{\text{bulk}}^L + \frac{1}{2}\{S_X^{(L)} + S_{\text{int}}^{(L)}\} + S_B^L] + S_H^{(L)} \\ &= 2[S_{\text{bulk}}^L + S_{X/2}^{(L)} + S_{\text{int}}^{(L)}|_{X/2} + S_B^L] + S_H^{(L)}. \end{aligned} \tag{7.2}$$

This reexpression reveals an alternative method to derive the fermion masses and couplings, which are independent from the pure scalar part, namely $S_H^{(L)}$. The idea is that, within the orbifold model now described by the action (7.2) importantly together with the description of the $\mathbb{Z}_2$ symmetry over $\mathcal{S}^1$, we can first search for the field parts along the limited domain $[0, \pi R]$. This search is in fact based on the action $[S_{\text{bulk}}^L + S_{X/2}^{(L)} + S_{\text{int}}^{(L)}|_{X/2} + S_B^L]$, since the overall factor 2 in Eq. (7.2) affects neither the EOM (global factor) nor the BC (same factor in front of the surface terms and pure brane terms combined into BC),[23] and is in turn strictly equivalent to solving the interval model. Given this action, the solutions obtained for the 4D masses (and 4D effective Yukawa coupling constants from profile overlaps with the

[23]This search could also be constrained by vanishing currents at $y = 0, \pi R$ instead of the S_B^L presence, in the free case, as shown in Secs. III B and V B.

Higgs boson peak at $y = \pi R$) are those of Ref. [38] but involving a normalized coupling parameter $X/2$. The last stage of this technics is the extension of the obtained profiles over the complete orbifold domain via the $\mathbb{Z}_2$ transformations, before applying the orthonormalization condition. The 4D effective Yukawa coupling constants are then changed by an additional factor $1/2$, as is clear from the dimensional wave function normalization forms (5.6)–(5.16), which confirms the result (5.21). On the other side, we see as well that the fermion masses so obtained (unchanged by the spatial domain extension) involve only a new normalized parameter $X/2$, with respect to Ref. [38], which confirms the found spectrum (5.20).

Beyond these action correspondences, there are other elegant similarities. For example, as illustrated by Fig. 4, both the interval and orbifold scenarios lead to the same vanishing probability current conditions at the two branes (and hence to identical EBC); those current conditions come, respectively, directly from the interval boundary criteria and indirectly from $\mathbb{Z}_2$ symmetry considerations. Besides, Table III shows that the same treatments of the two branes, at the fixed points or interval boundaries, must be adopted in identical situations and that the same BC are generated.

Finally, let us propose an intuitive description for understanding the orbifold versus interval model duality. The obtained wave functions for the bulk fermions on the interval are of the kind $\cos(M_n y) \propto (e^{iM_n y} + e^{-iM_n y})$, coming in factor (via the KK decomposition) of the energy coefficients $e^{\pm iEt}$ in the 4D Dirac fields, which gives rise to wave planes propagating in both y-directions of the interval with momenta $\pm p_n = \pm M_n$—as for oscillations left-moving and right-moving along opposite directions in the world-sheet parameter space of strings. The associated particle, going in the direction $L \to 0$ and then coming back along $0 \to L$, reproduces the propagation along $\mathcal{S}^1$, following consecutively the two fundamental domains $-\pi R \to 0^-$ and $0^+ \to \pi R$ of the orbifold (effectively equivalent orientations of the circle in the bulk so a unique propagation direction chosen along it): exactly the same $\mathcal{L}[\Phi(x^\mu, y)]$ Lagrangian evolution is felt by this particle during those dual travelings along the extra y-dimension, in the two different models, as is clear from the Lagrangian $\mathbb{Z}_2$ symmetry depicted in the drawing 1.

VIII. CONCLUSIONS

In the study of the $\mathcal{S}^1/\mathbb{Z}_2$ orbifold, the proper action definition through improper integrals has allowed to obtain consistent bulk profile solutions with possible discontinuities at the fixed points. In particular the point-like interaction of Yukawa creates a profile jump.

These solutions have been obtained without brane-Higgs regularization, by relying on the necessary EBC, coming from vanishing fermion probability currents, or alternatively on the introduction of BBT in the action. The associated calculations have been confirmed by the matching, between the 4D and 5D approaches, of the analytical results for the fermion mass spectrum and 4D effective Yukawa coupling constants.

The orbifold version, with $\mathbb{Z}_2$ transformations of the fields extended to the fixed points, was shown to be able to generate the chiral nature of the theory and even to select the expected SM chirality configuration for the 4D states.

The duality between the interval and orbifold scenarios has been deeply described. It has also constituted the opportunity to point out an alternative method for calculating the tower of excitation masses and 4D Yukawa couplings.

We are now working on the introduction of distributions in this context.

ACKNOWLEDGMENTS

R. L. is supported by the agreement signed between the *China Scholarship Council (CSC)* and the *Université Paris-Saclay.*

APPENDIX A: NOTATIONS AND CONVENTIONS

Throughout the paper, we use the conventions of Ref. [52]. The 5D Minkowski metric is,

$$\eta_{MN} = \mathrm{diag}(+1, -1, -1, -1, -1),$$

where $M, N = 0, 1, \ldots, 4$.

The 4D Dirac matrices are taken in the Weyl representation,

$$\gamma^\mu = \begin{pmatrix} 0 & \sigma^\mu \\ \bar{\sigma}^\mu & 0 \end{pmatrix} \quad \text{with} \quad \begin{cases} \sigma^\mu & = & (\mathbb{I}, \sigma^i), \\ \bar{\sigma}^\mu & = & (\mathbb{I}, -\sigma^i), \end{cases} \tag{A1}$$

where $\mu = 0, 1, 2, 3$ and σ^i ($i = 1, 2, 3$) are the three Pauli matrices:

$$\sigma^1 = \begin{pmatrix} 0 & 1 \\ 1 & 0 \end{pmatrix}, \quad \sigma^2 = \begin{pmatrix} 0 & -i \\ i & 0 \end{pmatrix}, \quad \sigma^3 = \begin{pmatrix} 1 & 0 \\ 0 & -1 \end{pmatrix}.$$

One has also the 4D chirality operator,

$$\gamma^5 = i \prod_{\mu=0}^{3} \gamma^\mu = \begin{pmatrix} -\mathbb{I} & 0 \\ 0 & \mathbb{I} \end{pmatrix}. \tag{A2}$$

In our conventions, the 5D Dirac matrices Γ^M ($M = 0, 1, \ldots, 4$) obey $\{\Gamma^A, \Gamma^B\} = 2\eta^{AB}$ ($A, B = 0, 1, \ldots, 4$) and read as,

$$\Gamma^M = (\gamma^\mu, -i\gamma^5). \tag{A3}$$

APPENDIX B: FROM SPINOR COMPONENTS TO COMPACT NOTATIONS

1. Spinor components and their variations

The generic spinor field F ($F = Q, D$) introduced via Eq. (2.6) can be written in terms of its four explicit components F_α [$\alpha = 1, 2, 3, 4$]:

$$F = \begin{pmatrix} F_1 \\ F_2 \\ F_3 \\ F_4 \end{pmatrix}, \tag{B1}$$

and similarly, $\bar{F}$ can be expressed in terms of its own four components $\bar{F}_\alpha$:

$$\begin{aligned} \bar{F} &= (\,\bar{F}_1, \quad \bar{F}_2, \quad \bar{F}_3, \quad \bar{F}_4\,) \\ &\hat{=}\, F^\dagger \gamma^0 = (\,F_3^*, \quad F_4^*, \quad F_1^*, \quad F_2^*\,). \end{aligned} \tag{B2}$$

These 8 components constitute the fundamental variables of the Lagrangian (2.5). Hence, the variation of the associated action, S_{bulk} [see Eq. (2.4)], involves the following 8 elementary variations, that we can group into new 4-component (transposed) vectorial objects defined as:

$$\delta F \hat{=} \begin{pmatrix} \delta F_1 \\ \delta F_2 \\ \delta F_3 \\ \delta F_4 \end{pmatrix}, \qquad \delta\bar{F} \,\hat{=}\, (\,\delta\bar{F}_1, \quad \delta\bar{F}_2, \quad \delta\bar{F}_3, \quad \delta\bar{F}_4\,), \tag{B3}$$

introducing the 8 components δF_α and $\delta\bar{F}_\alpha$. We then define,

$$\delta F = \begin{pmatrix} \delta F_L \\ \delta F_R \end{pmatrix},$$

$$\delta\bar{F} \hat{=} (\,\delta F_R^\dagger, \quad \delta F_L^\dagger\,), \text{with for instance, } \delta F_R^\dagger \hat{=} (\,\delta\bar{F}_1, \quad \delta\bar{F}_2\,), \tag{B4}$$

inspired by the following generic relations, based on Eq. (2.6),

$$F = \begin{pmatrix} F_L \\ F_R \end{pmatrix}, \qquad \bar{F} \,\hat{=}\, F^\dagger \gamma^0 = (F_R^\dagger, F_L^\dagger). \tag{B5}$$

2. A typical compact form calculation

Using the Lagrangian $\mathcal{L}_{\mathrm{kin}}$ of Eq. (2.5), let us work out explicitly the following quantity entering Eq. (3.1) in a compact form (no explicit spinor index of type α),

$$\begin{aligned} \delta\bar{F}\frac{\partial\mathcal{L}_{\mathrm{kin}}}{\partial\bar{F}} \hat{=} \sum_{\alpha=1}^{4}\delta\bar{F}_\alpha\frac{\partial\mathcal{L}_{\mathrm{kin}}}{\partial\bar{F}_\alpha} &= \sum_{\alpha=1}^{4}\delta\bar{F}_\alpha\frac{\partial}{\partial\bar{F}_\alpha}\left(\frac{i}{2}\bar{F}\Gamma^M\partial_M F\right) \\ &= \sum_{\alpha=1}^{4}\delta\bar{F}_\alpha\frac{\partial}{\partial\bar{F}_\alpha}\left(\frac{i}{2}\sum_{\beta=1}^{4}\bar{F}_\beta[\Gamma^M\partial_M F]_\beta\right) \\ &= \sum_{\alpha=1}^{4}\delta\bar{F}_\alpha\frac{i}{2}[\Gamma^M\partial_M F]_\alpha \\ &= \frac{i}{2}\delta\bar{F}\Gamma^M\partial_M F, \end{aligned} \tag{B6}$$

where the spinor components of Eqs. (B1) and (B2) have appeared, as well as the variations of Eq. (B3).

3. $\mathbb{Z}_2$ transformations of field variations

Finally, we can derive the $\mathbb{Z}_2$ transformation for the compact form $\delta\bar{F}$ of Eq. (B3). Accordingly to the $\mathbb{Z}_2$ transformations (2.7)–(2.10), we have,

$$\begin{aligned} \bar{F}|_{-y} = F^\dagger|_{-y}\gamma^0 &= (\pm\gamma^5 F)^\dagger|_y\gamma^0 = \pm F^\dagger|_y\gamma^5\gamma^0 \\ &= \mp F^\dagger|_y\gamma^0\gamma^5 = \mp\bar{F}|_y\gamma^5, \end{aligned}$$

due to the anticommutator relation $\{\gamma^5, \gamma^\mu\} = 0$. Then one must rewrite this relation by making the spinor components of Eq. (B2) appear explicitly:

$$\bar{F}_\alpha|_{-y} = \mp\sum_{\beta=1}^{4}\bar{F}_\beta|_y\gamma^5_{\beta\alpha},$$

in order to deduce the relation on the variations of these components:

$$\delta\bar{F}_\alpha|_{-y} = \mp\sum_{\beta=1}^{4}\delta\bar{F}_\beta|_y\gamma^5_{\beta\alpha}.$$

Thanks to Eq. (B3), this equation can be contracted back to the compact notation as,

$$\delta\bar{F}|_{-y} = \mp\delta\bar{F}|_y\gamma^5. \tag{B7}$$

[1] L. Randall and R. Sundrum, Large Mass Hierarchy from a Small Extra Dimension, Phys. Rev. Lett. **83**, 3370 (1999).
[2] S. Chang, J. Hisano, H. Nakano, N. Okada, and M. Yamaguchi, Bulk standard model in the Randall-Sundrum background, Phys. Rev. D **62**, 084025 (2000).
[3] T. Gherghetta and A. Pomarol, Bulk fields and supersymmetry in a slice of AdS, Nucl. Phys. **B586**, 141 (2000).
[4] S. J. Huber and Q. Shafi, Neutrino oscillations and rare processes in models with a small extra dimension, Phys. Lett. B **512**, 365 (2001).
[5] S. Casagrande, F. Goertz, U. Haisch, M. Neubert, and T. Pfoh, Flavor physics in the Randall-Sundrum model: I. Theoretical setup and electroweak precision tests, J. High Energy Phys. 10 (2008) 094.
[6] S. Chang, C. S. Kim, and M. Yamaguchi, Hierarchical mass structure of fermions in warped extra dimension, Phys. Rev. D **73**, 033002 (2006).
[7] G. Moreau and J. I. Silva-Marcos, Neutrinos in warped extra dimensions, J. High Energy Phys. 01 (2006) 048.
[8] G. Moreau and J. I. Silva-Marcos, Flavor physics of the RS model with KK masses reachable at LHC, J. High Energy Phys. 03 (2006) 090.
[9] C. Bouchart and G. Moreau, The precision electroweak data in warped extra-dimension models, Nucl. Phys. **B810**, 66 (2009).
[10] F. Englert and R. Brout, Broken Symmetry and the Mass of Gauge Vector Mesons, Phys. Rev. Lett. **13**, 321 (1964).
[11] P. W. Higgs, Broken symmetries, massless particles and gauge fields, Phys. Lett. **12**, 132 (1964).
[12] K. R. Dienes, E. Dudas, and T. Gherghetta, Neutrino oscillations without neutrino masses or heavy mass scales: A higher dimensional seesaw mechanism, Nucl. Phys. **B557**, 25 (1999).
[13] A. Abada, P. Dey, and G. Moreau, Neutrinos in flat extra dimension: Towards a realistic scenario, J. High Energy Phys. 09 (2007) 006.
[14] Y. Grossman and M. Neubert, Neutrino masses and mixings in nonfactorizable geometry, Phys. Lett. B **474**, 361 (2000).
[15] S. J. Huber and Q. Shafi, Majorana neutrinos in a warped 5-D standard model, Phys. Lett. B **544**, 295 (2002).
[16] G. Moreau, Realistic neutrino masses from multi-brane extensions of the Randall-Sundrum model?, Eur. Phys. J. C **40**, 539 (2005).
[17] J. M. Frère, G. Moreau, and E. Nezri, Neutrino mass patterns within the seesaw model from multilocalization along extra dimensions, Phys. Rev. D **69**, 033003 (2004).
[18] F. Nortier, Large star/rose extra dimension with small leaves/petals, Int. J. Mod. Phys. A **35**, 2050182 (2020).
[19] F. Ledroit, G. Moreau, and J. Morel, Probing RS scenarios of flavour at LHC via leptonic channels, J. High Energy Phys. 09 (2007) 071.
[20] C. Bouchart and G. Moreau, Higgs boson phenomenology and vacuum expectation value shift in the Randall-Sundrum scenario, Phys. Rev. D **80**, 095022 (2009).
[21] A. Djouadi, G. Moreau, and F. Richard, Resolving the A (FB)**b puzzle in an extra dimensional model with an extended gauge structure, Nucl. Phys. **B773**, 43 (2007).
[22] A. Djouadi, G. Moreau, and R. K. Singh, Kaluza-Klein excitations of gauge bosons at the LHC, Nucl. Phys. **B797**, 1 (2008).
[23] A. Djouadi and G. Moreau, Higgs production at the LHC in warped extra-dimensional models, Phys. Lett. B **660**, 67 (2008).
[24] A. Djouadi, G. Moreau, F. Richard, and R. K. Singh, The forward-backward asymmetry of top quark production at the Tevatron in warped extra dimensional models, Phys. Rev. D **82**, 071702 (2010).
[25] A. Djouadi, G. Moreau, and F. Richard, Forward-backward asymmetries of the bottom and top quarks in warped extra-dimensional models: LHC predictions from the LEP and Tevatron anomalies, Phys. Lett. B **701**, 458 (2011).
[26] A. Angelescu, G. Moreau, and F. Richard, Scalar production in association with a Z boson at the LHC and ILC: The mixed Higgs-radion case of warped models, Phys. Rev. D **96**, 015019 (2017).
[27] C. Bouchart, A. Knochel, and G. Moreau, Discriminating 4D supersymmetry from its 5D warped version, Phys. Rev. D **84**, 015016 (2011).
[28] J. Polchinski, Tasi lectures on D-branes, in Fields, strings and duality, in *Proceedings, Summer School, Theoretical Advanced Study Institute in Elementary Particle Physics, TASI'96, Boulder, USA, 1996* (1996), pp. 293–356 [arXiv:hep-th/9611050].
[29] C. P. Bachas, Lectures on D-branes, in duality and supersymmetric theories, in *Proceedings, Easter School, Newton Institute, Euroconference, Cambridge, UK, 1997* (1998), pp. 414–473, https://arxiv.org/abs/hep-th/9806199.
[30] O. Aharony, S. S. Gubser, J. M. Maldacena, H. Ooguri, and Y. Oz, Large N field theories, string theory and gravity, Phys. Rep. **323**, 183 (2000).
[31] M. J. Duff, Supermembranes, in 26th British Universities Summer School in Theoretical Elementary Particle Physics (BUSSTEPP 1996) Swansea, Wales, 1996.
[32] S. Fichet, Braneworld effective field theories—Holography, consistency and conformal effects, J. High Energy Phys. 04 (2020) 016.
[33] F. Nortier, Consistency of Braneworld effective field theories, arXiv:2007.04266.
[34] L. J. Dixon, J. A. Harvey, C. Vafa, and E. Witten, Strings on orbifolds, Nucl. Phys. **B261**, 678 (1985).
[35] L. J. Dixon, J. A. Harvey, C. Vafa, and E. Witten, Strings on orbifolds. 2., Nucl. Phys. **B274**, 285 (1986).
[36] M. Quiros, New ideas in symmetry breaking, in *Summer Institute 2002 (SI 2002) Fuji-Yoshida, Japan, 2002* (2003), pp. 549–601 [arXiv:hep-ph/0302189].
[37] K.-S. Choi and J. E. Kim, *Quarks and Leptons From Orbifolded Superstring*, Vol. 954 (Springer, Cham, 2020), 10.1007/978-3-030-54005-0.
[38] A. Angelescu, R. Leng, G. Moreau, and F. Nortier, Beyond brane-Higgs regularization: Clarifying the method and model, Phys. Rev. D **101**, 075048 (2020).
[39] F. Nortier, Compactified spacelike extra dimension & Brane-Higgs field, Ph.D. thesis, Université Paris-Saclay, arXiv:2005.00292.
[40] J. Scherk and J. H. Schwarz, How to get masses from extra dimensions, Nucl. Phys. **B153**, 61 (1979).
[41] E. Cremmer, J. Scherk, and J. H. Schwarz, Spontaneously broken $N = 8$ supergravity, Phys. Lett. **84B**, 83 (1979).
[42] T. Gherghetta and A. Pomarol, A warped supersymmetric standard model, Nucl. Phys. **B602**, 3 (2001).

[43] C. Csaki, C. Grojean, J. Hubisz, Y. Shirman, and J. Terning, Fermions on an interval: Quark and lepton masses without a Higgs, Phys. Rev. D **70**, 015012 (2004).

[44] A. Azatov, M. Toharia, and L. Zhu, Higgs mediated FCNC's in warped extra dimensions, Phys. Rev. D **80**, 035016 (2009).

[45] A. Azatov, O. Bondu, A. Falkowski, M. Felcini, S. Gascon-Shotkin, D. Ghosh, G. Moreau, A. Y. Rodríguez-Marrero, and S. Sekmen, Higgs boson production via vector-like top-partner decays: Diphoton or multilepton plus multijets channels at the LHC, Phys. Rev. D **85**, 115022 (2012).

[46] N. Bonne and G. Moreau, Reproducing the Higgs boson data with vector-like quarks, Phys. Lett. B **717**, 409 (2012).

[47] G. Moreau, Constraining extra-fermion(s) from the Higgs boson data, Phys. Rev. D **87**, 015027 (2013).

[48] S. Gopalakrishna, T. Mandal, S. Mitra, and G. Moreau, LHC signatures of warped-space vectorlike quarks, J. High Energy Phys. 08 (2014) 079.

[49] A. Angelescu, A. Djouadi, and G. Moreau, Vector-like top/bottom quark partners and Higgs physics at the LHC, Eur. Phys. J. C **76**, 99 (2016).

[50] K. Agashe, A. Delgado, M. J. May, and R. Sundrum, RS1, custodial isospin and precision tests, J. High Energy Phys. 08 (2003) 050.

[51] M. E. Peskin and D. V. Schroeder, *An Introduction to Quantum Field Theory* (Addison-Wesley, Reading, MA, 1995).

[52] M. D. Schwartz, *Quantum Field Theory and the Standard Model* (Cambridge University Press, Cambridge, England, 2014).

[53] R. Barceló, S. Mitra, and G. Moreau, On a boundary-localized Higgs boson in 5D theories, Eur. Phys. J. C **75**, 527 (2015).